8-6-2021

The role of a sickled microenvironment in cardiac dysfunction

Allison Nicole Healey
ahealey15@gmail.com

The role of a sickled microenvironment in cardiac dysfunction

By

Allison Nicole Healey

Approved by:

C. LaShan Simpson (Major Professor)
Alicia Olivier
Steven H. Elder
Steven H. Elder (Graduate Coordinator)
Jason M. Keith (Dean, Bagley College of Engineering)

A Thesis
Submitted to the Faculty of
Mississippi State University
in Partial Fulfillment of the Requirements
for the Degree of Master of Science
in Biomedical Engineering
in the Department of Agricultural and Biological Engineering

Mississippi State, Mississippi

August 2021

Name: Allison Nicole Healey

Date of Degree: August 6, 2021

Institution: Mississippi State University

Major Field: Biomedical Engineering

Major Professor: C. LaShan Simpson

Title of Study: The role of a sickled microenvironment in cardiac dysfunction

Pages in Study: 63

Candidate for Degree of Master of Science

This study helps to fill a remaining knowledge gap surrounding the mechanisms and pathways that contribute to cardiomyopathies in SCD. A better understanding of the pathophysiological mechanisms could lead to more accurate therapeutic targets to improve quality of life as well as life expectancy. In this study I recapitulate cardiac dysfunction *in vitro* by exposing engineered mouse cardiac tissues to ANG II or the sickled microenvironment.

Experimental results include gene expression profiles and oxidative stress generation. Gene expression profiles in the ANG II treated tissues indicated a pathological state with upregulation in biomarkers for inflammation, cell adhesion, wall stress and ECM related genes. Further research is being conducted using insights gained from this study which will lead to a broader understanding of the biological processes involved and potentially identify novel therapeutic targets that may ultimately improve patient outcomes.

DEDICATION

I would like to dedicate this study to my family who have supported through this process.

I could not have accomplished this without the constant love and support from Eli, Benji and Teddy.

ACKNOWLEDGEMENTS

I would like to personally thank and acknowledge the faculty and staff at Mississippi State University for their support of my research. First and foremost, I would like to acknowledge my advisor, Dr. Renita E. Horton for her patience, assistance and guidance through my time at MSU. Second, I would like to thank Dr. C. LaShan Simpson for her support and guidance along the way. Additionally, I thank Dr. Elder for his assistance and time. I thank Dr. Olivier for providing invaluable feedback. I would also like to thank Dr. Santanu Kundu for his assistance and laboratory access. Lastly, I would like to thank the past members of the Cardiovascular Tissue Engineering Laboratory, specifically, Kristen Hubbard, Jackson Coole and Olamide Lewis for their daily assistance and support.

TABLE OF CONTENTS

LIST OF TABLES

LIST OF FIGURES

CHAPTER I

INTRODUCTION: SICKLE CELL DISEASE

1.1 Motivation

Sickle cell disease (SCD) is an inherited genetic disorder that is caused by a mutation in the □-globin gene leading to pathophysiological consequences. In 1910, Dr. James Herrick reported the first recognition of SCD, through his description of irregularly shaped red blood cells as a "large number of thin, elongated sickle-shaped and crescent-shaped forms" [1] Unfortunately, due to high infant mortality rates and vulnerability to infectious diseases, the disease was rarely diagnosed for several decades. Nearly 50 years after Herrick's report, Pauling and Itano, established SCD as a molecular disease [2]. During the 1960's the disease became a political symbol for equal rights of black Americans. In response to the increased social awareness, comprehensive SCD centers were established in the USA during the 1970's. Subsequently by 1994, the median age of death rose from less than 20 years or age to 48 and 42 years of age, in women and men, respectfully. Through advances in comprehensive care and the introduction of hydroxyurea, survival to 18 years of age reached 96% in 2010 [3]–[7]. Despite the improved survival for children and adolescents, adult SCD-related mortality may have increased. The centers for disease control and prevention's (CDC) sickle cell data collection (SCDC) program found the most frequent and severe symptoms occurred during the transition from pediatric to adult care. A recent study reported patients 20-25 years of age exhibit two times the mortality than patients 15-19 years of age. SCD continues to be associated with poor

outcomes with major consequences of cardiac morbidity, early mortality, and sudden death. Through a better understanding of the pathophysiology of SCD, more accurate therapeutic targets can be distinguished to improve not only life expectancy, but also the quality of life. Through the use of a physiologically relevant *in vitro* platform, this study will help to fill remaining knowledge gaps surrounding the mechanisms and pathways that contribute to cardiomyopathies in conjunction with SCD.

1.2 Genetics

1.2.1 Hemoglobin

Hemoglobin is a vital protein found in most vertebrates as well as some invertebrates. It is the main protein in mature red blood cells (RBC) and functions as the oxygen carrying component. Hemoglobin is a tetramer composed of four globin subunits. Each globin subunit is associated with a heme thus allowing a molecule of oxygen to bind to each subunit [8].Consequently, hemoglobin has an increased oxygen-transport from the lungs to the remainder of the body for cellular respiration [8]. There are at least six genes that encode various types of globin subunits thus generating variations of the hemoglobin tetramer.

Fetal hemoglobin (HbF) is the heterodimeric combination of two alpha-globin and two gamma-globin proteins [9]. HbF is the predominant hemoglobin type after the first trimester of gestation and is gradually replaced by adult hemoglobin shortly after birth [10]. From birth through the first several months of life, the presence of high levels of HbF protect against vaso-occclusive events and hemolytic features of SCD [11]. In adults, HbF generally compromises less than 1% of total hemoglobin [12].

Newborns undergo a transition from fetal hemoglobin (HbF) to adult hemoglobin (HbA). HbA is the preeminent expression of hemoglobin in healthy adults. This molecule is composed of two alpha-globin subunits and two beta-globin subunits [13].

Hemoglobin A2 (HbA_2) is less common HbA accounting for approximately 3% in healthy adults. There is no known physiological relevance of HbA2 however, elevated levels have been associated with individuals with sickle cell disease and other hematologic disorders [14].

Sickled hemoglobin (HbS) is the result of a single nucleotide substitution in the HBB gene that encodes for HbA beta-globin subunits. When a hemoglobin protein contains this point mutation it is considered to be hemoglobin S [2], [7], [15]. Each parent contributes one copy of the HBB gene, thus everyone recieves two copies of the HBB gene. The most severe form of sickle cell disease (SCD), sickle cell anemia (SCA), occurs when an individual is homozygous for HbS, meaning they have inherited HbS from each parent. Variations in SCD are the result of a combination of a single HbS gene and other abnormal hemoglobin genes. The different types of SCD include hemoglobin SC, SD, SE and S□ thalassemia. These variations are normally less severe and uncommon than SCA. Heterozygous individuals, expressing one normal and one abnormal gene are considered to carry the sickle cell trait (SCT). These individuals produce HbA and HbS as the oxygen bearing molecules in their RBCs. Typically, SCT individuals are considered asymptomatic, however SCT has been associated with other cardiovascular complications, morbidities, and mortalities. Additional research needs to be conducted to elucidate the extent [4], [16], [17].

1.3 Pathophysiology

The pathophysiology of sickle cell disease (SCD) is predicated on the polymerization of HbS as a result of low-oxygen tension. Hemoglobin polymerization affects the structure, physical and biochemical properties of red blood cells (RBCs), including increased adhesion, stiffness, morphology, and oxidative damage. Compared to HbA, HbS has reduced oxygen affinity [18]. This reduced oxygen affinity exhibited in HbS exacerbates HbS polymerization which in turn creates a positive feedback look further reducing the oxygen affinity of HbS. Upon polymerization the structure of the RBCs physically deforms from the typical biconcave shape into a sickled shape. This deformation leads to increased stiffness and impaired rheology of RBC. Repeated cycles of polymerization and sickling in low oxygen conditions eventually results in permanent damage to the RBC leaving the cell in an irreversible sickled state.

The increased adhesion seen in RBCs containing HbS causes the cells to adhere to the post-capillary venule thus narrowing the lumen diameter. The blood flow velocity is inversely proportional to the diameter of the blood vessel lumen. This combined with the increased stiffness of sickled RBCs further impairs blood flow rheology and eventually leads to the formation of vaso-occlusion.

Not only do HbS polymerization and vaso-occlusion play- crucial roles in the development of the pathophysiology of SCD, they are also responsible for precipitating a cascade of subsequent pathologic events and complications including endothelial dysfunction, depletion of nitric oxide (NO) bioavailability, and oxidative stress. The direct contact between the sickled RBCs and endothelial cells (EC) leads to endothelial activation and dysfunction. Endothelial cells line the inner surface of lymphatic and blood vessels and perform important functions in regard to the development and maintenance of vascular tone, nutrient exchange,

organ development, and blood fluidity. The abnormal RBC to EC interaction leads to dysfunction of the vascular endothelium that contributes to the overall vascular pathophysiology of SCD, specifically vaso-occlusions and chronic organ damage [19]–[21]. The endothelial dysfunction observed in SCD can be characterized by a change in the processes of the endothelium to a state of reduced vasodilatory responses, a proinflammatory state and prothrombic properties. upregulation of adhesion molecules. The mechanisms involved in this change include reduced nitric oxide production, increased oxidative stress, as well as upregulation of adhesion molecules such as vascular cell adhesion molecule 1 (VCAM-1) and intercellular adhesion molecule 1 (ICAM-1) as well as inflammatory mediators like interleukin 6 (IL-6).

Nitric oxide is an important regulator of vascular homeostasis and vasodilation. In SCD there is a depletion of NO bioavailability. This is largely contributed to the1000-fold increase in plasma hemoglobin released from hemolyzed RBC scavenging NO as compared to cytoplasmic hemoglobin [22]. Reduced NO bioactivity can impair the regulation of blood flow and promote RBC adhesion thereby contributing to the occlusive process. Reactive oxygen species (ROS) scavenge NO further reducing NO bioavailability.

It is believed that the leading source of free radical production in SCD is a result of the reoxygenation phase of RBC. During reoxygenation, RBCs generate superoxide as a byproduct of reaction between heme iron and oxygen. In contrast to HbA, HbS becomes overwhelmed by the perpetual source of superoxide and hydrogen peroxide. Compared to HbA, sickled cells develop approximately twofold greater quantities of superoxide, hydrogen peroxide and hydroxyl radicals. When hydrogen peroxide is exposed to methemoglobin, it decomposes hemoglobin and releases iron. The iron released then reacts with residual hydrogen peroxide to

produce additional hydroxyl radicals. When ROS are not neutralized through ROS defense mechanisms such as, enzymatic antioxidants, like NO, or through nonenzymatic antioxidants such as reduced glutathione (GSH), the oxidative stress can result in increased endothelial cell adhesion and cell destruction [18]. Furthermore, the oxidative stress oxidizes the intracellular enzyme target of NO, soluble guanylate cyclase (sGC), rendering it inactive. In its active state, sGC catalyzes the synthesis of cyclic guanosine monophosphate, which in turn promotes vasodilation and inhibits smooth muscle proliferation [20]. Thus by disrupting the NO-sGC signaling mechanism, oxidative stress leads to vascular dysfunction [23].

1.4 Clinical Manifestations

Sickle cell disease manifest in a variety of symptoms including, but not limited to pain, anemia, infection, myocardial infarction and fibrosis. The most common clinical manifestation of SCD is referred to as pain crisis or vaso-occlusive crisis (VOC). These painful crises are a result of vascular sickling and hemolysis. Painful crises are often precipitated by a variety of factors including infection, cold weather and dehydration. Patients with SCD have increased susceptibility to infection due to their impaired immunity. The impaired immunity is partially due to autosplenectomy.

The spleen plays an important function in immune defense and quality control of altered RBCs. In SCD the first organ injured is typically the spleen due to recurring vaso-occlusive infarctions in the spleen that leads to fibrosis and autosplenectomy [24]. Consequently, there is an increased susceptibility to infection. Infection is one of the major complications of sickle cell disease and is associated with morbidities and mortalities [13], [25]. In children, infection is the leading cause of premature deaths [26], [27]. Malaria, pneumococcal and haemophilus infections

are all believed to contribute to the increased morbidity and mortality.

Cardiopulmonary complications are the major complications in individuals surviving to adulthood with SCD. Patients with SCD have a unique cardiac pathophysiology characterized by a restrictive physiology that is superimposed on features of hyperdynamic circulation. In SCD, the primary characteristics of the restrictive cardiomyopathies are diastolic dysfunction, left atrial (LA) dilation, and left ventricular (LV) enlargement [20], [27], [28]. In addition, myocardial tissue specimens displayed an increased heart weight, myocardial fibrosis and pulmonary vascular changes. Figures 1.1 and 1.2 compare the progression of fibrosis and heart to body mass ratio in healthy and diseased mice using the Townes mouse model. In the Townes mouse model, genes are knocked-in replacing endogenous mouse α-globin genes with human α-globin genes and endogenous mouse β globin genes with human Aγ and β^s globin genes [29]. It is believed that LV diastolic dysfunction is primarily associated with increased aortic stiffness while myocardial fibrosis is correlated with increased blood transfusion requirements [30].

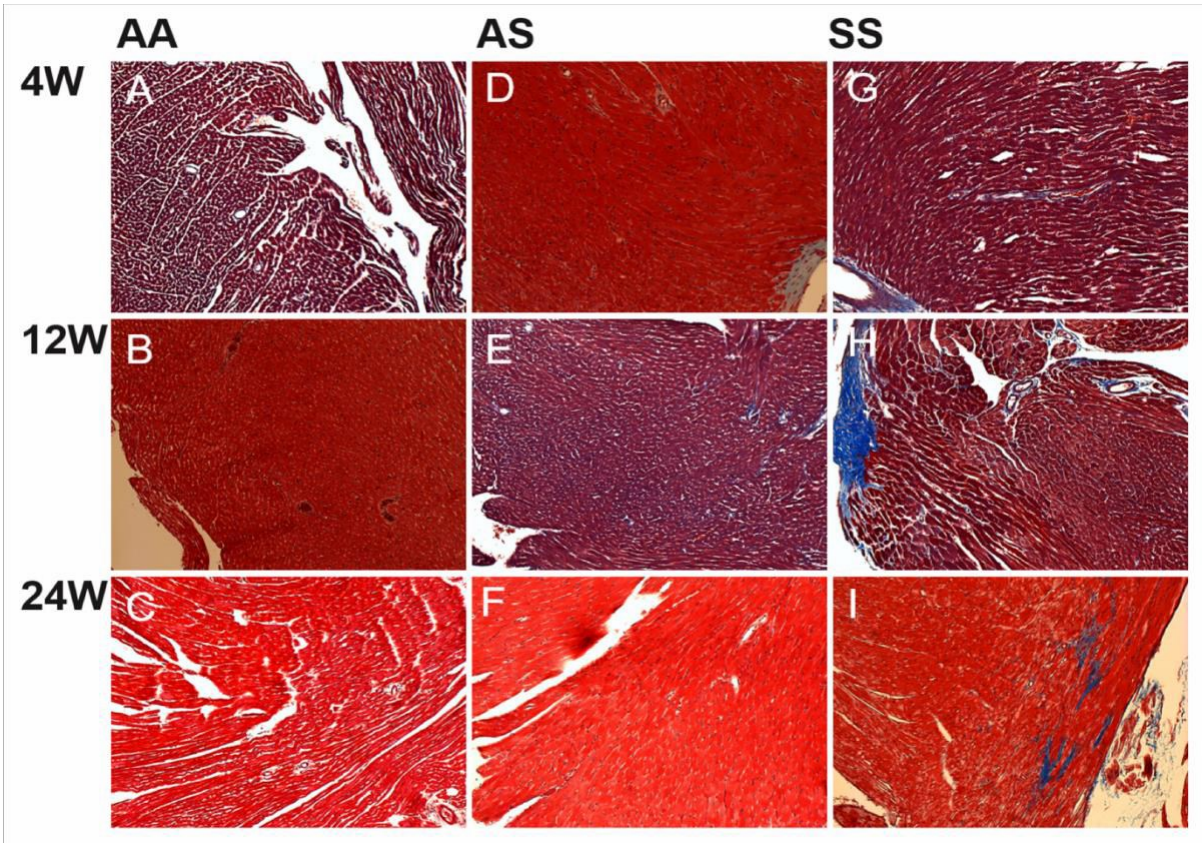

Figure 1.1 Masson's Trichrome Stained Townes Mice Hearts

Progression of fibrosis seen in genetically modified Townes mice. Mice were bred and phenotyped for control (HbAA), sickle trait (HbAS), and sickle cell anemia (HbSS) human hemoglobins Scale bar = 100 □m

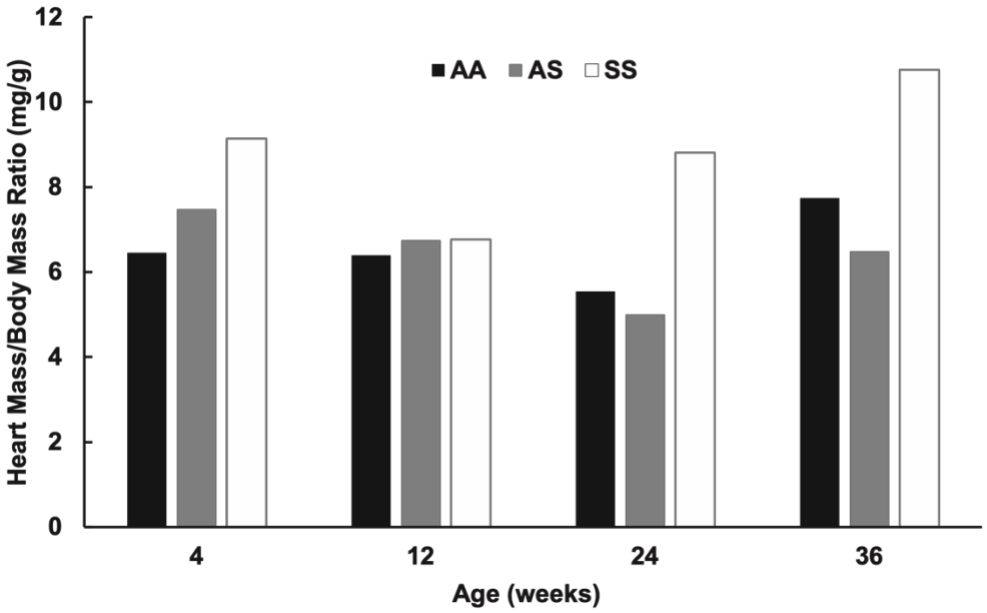

Figure 1.2 Heart to Body Ratio of Townes Mice

Heart to body ratio from 4-36 weeks of Townes mice bred and phenotyped for control (HbAA), sickle trait (HbAS), and sickle cell anemia (HbSS) human hemoglobins. N = 42

Outside of painful crises, acute chest syndrome (ACS) is the most frequent reason for hospitalization and is the leading cause of death in individuals with SCD. Over 10% of adult cases of ACS are fatal or complicated by multi-organ failure and neurological events [13]. The initial pulmonary injury is caused by a number of factors including infection, pulmonary infarction, sickle cells blocking blood vessels, surgical procedures and pulmonary embolism [28]. At the pulmonary endothelial cell level, the imbalance of NO to adhesive forces leads to increase intrapulmonary sickle cell adhesion.

1.5 Clinical Treatment

Sickle cell disease is treated in a variety of ways based on the severity and symptoms present. The most common cause of hospitalization is a result of severe pain from the condition. Discussed below are the most relevant and promising therapies related to SCD.

1.5.1 Pain Management

Pain is considered to be one of the major consequences of SCD. Patients can begin to suffer pain as early as infancy with increased severity throughout life. The combination of acute pain as well as chronic pain can result in poor quality of life and hospitalization. There are two main approaches to treat pain related to SCD. These strategies include analgesics that target the central nervous system (CNS) and implementing disease-modifying therapies to treat the sickle pathobiology and underlying pain [31], [32]. Currently, opioids are the most common treatments for moderate to severe pain in SCD. Unfortunately, long term use can lead to adverse side effects. Opioids negatively alter RBC deformability, rheology, membrane structure and dehydration. In addition, the binding of analgesic opioids such as morphine, fentanyl and hydromorphone, to μ-opioid receptors activates several signaling pathways that can amplify complications. These complications include but are not limited to endothelial activity, vascular permeability, stroke, hyperalgesia, opioid tolerance, renal pathology and retinopathy. A study conducted using the Berkley sickled mice model investigated the influence of chronic morphine use and demonstrated notable renal pathology and impaired renal function [33].

Due to the severity of the side effects that can arise from chronic opioid use, alternatives pain management therapies are being investigated. Cannabis offers a novel approach for the treatment of pain and possible hyperalgesia. Cannabis has already proven an effective alternative

in treating pain associated with HIV, multiple sclerosis and cancer. The BERK sickle mice model has been used to investigate the effects of systemic administration of cannabis in SCD. Administration of cannabis attenuated deep tissue hyperalgesia in sickle cell mice [33]. Currently 33 states and Washington D.C. have medical marijuana laws. At least 5 of these states have approved SCD as a qualifying condition. Subsequently, retrospective studies have been completed using the results of urine drug screen tests in adults with SCD. The results found no significant difference in the amounts of opioids consumed between cannabis users versus nonusers [34]. Additional human trials will need to be completed to clarify the effect and role of cannabis for SCD treatment. Alternatively, some individuals have also found relief through the use of nonpharmacological interventions such as massage, acupuncture, and self-relaxation techniques [34]. In addition, physicians and caregivers recommend preventative measures and therapies to avoid crisis triggers.

1.5.2 Approved Drug Therapies

1.5.2.1 Hydroxyurea

Hydroxyurea (HU) or hydroxycarbamide, is a ribonucleotide reductase inhibitor first approved for use by the Food and Drug Administration (FDA) in 1998 and by the European Medicines Agency (EMA) in 2007 for treatment of SCD. Through a mechanism that is not fully understood, HU increases cGMP levels thereby increasing the expression of HbF and decreasing leukocyte count [13]. The increased expression of HbF in turn reduces the concentration of HbS in RBCs [35]. As a result of the increased HbF concentration within their RBCs, individuals experience milder disease symptoms such as milder anemia as well as a reduction in the frequency and severity of VOCs [35], [36]. Furthermore, HU may function as an anti-

inflammatory due to the generation of nitric oxide. Unfortunately, HU is associated with a variety of side effects and concerns have been raised concerning toxicity and the long-term effects. Thus there continues to be a need for the identification and development of therapeutics to be used in conjunction with or in place of HU [37]–[40].

1.5.2.2 Glutamine

Glutamine is an influential amino acid involved in the synthesis and production of arginine, nicotinamide adenine dinucleotide (NAD), and glutathione (GSH). These substances are used to combat oxidative damage [20]. In SCD there is an increase in free radicals and oxidative damage. Similarly, to hydroxyurea, the exact mechanism of action of L-glutamine is unknown. It is thought to act as an antioxidant agent in SCD by preserving NADPH levels necessary for GSH recycling [41]. The FDA approved oral administration of L-glutamine, Endari, to treat SCD in 2017 after successful completion of phase 2 and phase 3 clinical trials [42]. The results from these trials showed a reduction in the frequency of painful crises as well as a reduction in emergency department visits [43] Currently, Endari is only approved for use in patients five years of age or older. Unlike hydroxyurea, Endari does not directly target VOs, instead Endari is used as a preventative treatment to reduce the severity as well as frequency of VOCs.

1.5.3 Pharmacologic Therapies Under Investigation

Although only two drug therapies have been approved for treatment of SCD, numerous therapeutic targets are being investigated. The increased understanding of the complexity and

multiplicity of the pathophysiology of SCD has led to the new therapeutic strategies. Therapeutic targets under investigation include but are not limited to agents that augment NO bioavailability (or its targets), target cellular adhesion, platelet aggregation or coagulation, and inhibit hemoglobin polymerization [41], [44], [45].

1.5.3.1 Therapeautics that Augment NO Bioavailability or NO Targets

As previously mentioned, the NO-sGC signaling pathway plays a crucial role in the physiology of the cardiovascular system, specifically in relation to vasodilation. When NO binds to heme it activates the catalytic domain on sGC which enables the synthesis of of cGMP from guanosine triphosphate (GTP). Impaired NO signaling and altered NO-cGMP homeostasis are considered hallmarks of cardiovascular diseases and are thus important therapeutic targets [46]. Multiple therapeutic strategies have been investigated to combat the reduced NO bioavailability observed in SCD. Preliminary studies of inhaled NO gas demonstrated some therapeutic effects in patients suffering from acute VOCs [45], [47]–[50]. However, a subsequent larger double-blind, placebo-controlled study in 150 patients hospitalized with VOC yielded no clinically significant effects of inhaled NO [45], [46], [51]. L-arginine has been studied as another strategy to promote NO bioavailability[45], [46], [51]–[54]. Reduced arginine levels are considered a rate-limiting step for NO production during VOC. Oral administration of L-arginine in conjunction with HU demonstrated an increase in nitrate levels. Additionally, in a double-blind placebo-controlled trial on 38 children with SCD, L-arginine administration corresponded with reduced opioid us and lower pain scores [55].

The sustained mechanisms that constrict NO production and bioavailability are likely responsible for the limited efficacy of NO inhalation and L-arginine supplementation on NO-

sGC signaling restoration. As an alternative, the molecular target of NO, sGC, has been investigated [23], [46], [51], [56], [57]. The target of two classes of sGC therapeutics are heme-dependent sGC stimulators and heme-independent activators. The sGC stimulators not only interact with endogenously available NO but are also capable of direct binding and stimulation of sGC to synthesize cGMP independently of NO. Riociguat and Olinciguat are two such sGC stimulators currently being investigated [51], [58]. In 2013, Riociguat was approved for the treatment of of pulmonary hypertension. A phase 2 double-blind, placebo-controlled study (NCT02633397) is currently being conducted to evaluate the safety, tolerability and efficacy in patients with SCD. Study completion is estimated in June of 2022. It should be noted, due to the short half-life of Riociguat thrice-daily dosing is required. In contrast, Olinciguat is a once-daily dose. In a phase 1b placebo-controlled study, olinciguat increased plasma cGMP levels and no serious adverse effects were observed [58]. Based upon the study, the FDA granted orphan drug status as a potential treatment for SCD. A phase 2 placebo-controlled, double-blind study (NCT03285178) in patients with SCD was completed in the summer of 2020. The results from this study have not be published yet.

1.5.3.2 Therapeutics That Target Cellular Adhesion

Vascular occlusion is thought to be the cause of the sickle cell pain crises. To combat vascular obstruction generated by the adhesion of sickled RBCs and white blood cells (WBC) to the endothelium anti-adhesive agents that target RBC and WBC endothelial interactions are being investigated [41], [44], [45]. The adhesion process in RBC and WBC is mediated by P- selectin thus making P-selectin inhibitors potential therapeutics. Crizanlizumab (SEG101) is a humanized monoclonal antibody that binds to P-selectin and prevents interaction with P-selectin glycoprotein

1 [59]. Completion of a 12-month, phase II placebo-controlled, double-blind safety and efficacy study, reported a 45.3% decrease in the frequency of crises per year [60]. No differences were observed in hemolytic parameters suggesting that the reduction in crises was due to the modified cellular adhesion. Based upon the findings of the study, the FDA granted Breakthrough Therapy designation to crizanlizumab in January of 2019 for the prevention of VOC in individuals with SCD. Pan-selectin inhibitors are also being investigated as anti-adhesive agents. Rivipansel (GMI-1070) is one such agent that inhibits cell-cell interactions and adhesion [41]. A phase 3 study (NCT02187003) to evaluate the efficacy and safety in patients 6 years of age or older suffering from a pain crisis related to SCD that requires hospitalization was completed in June of 2019. Results have yet to be published.

1.5.3.3 Therapeutics that Target Platelet Aggregation or Coagulation

Another avenue of interest includes therapies that target platelet activation and interaction inflammatory cells. Ticagrelor is a P2Y12 ADP receptor antagonist that has some influence on the vascular tone and inflammatory response. Ticagrelor is already an approved blood thinner but is now being investigated as a potential treatment for SCD [61]. A phase 3 clinical trial (NCT03615924) to investigate the effect of Ticagrelor in reducing the frequency of VOC in pediatric patients with SCD was terminated early following a recommendation from an independent data monitoring committee.

1.5.3.4 Therapeutics that inhibit Hemoglobin Polymerization

Example Paragraph Although the polymerization of HbS is considered the root cause of SCD, all of the previously mentioned therapies are directed towards the downstream

consequences of HbS polymerization, such as nitric oxide bioavailability, adhesion of RBC, and coagulation. Less attention has been devoted to the investigation of preventing or limiting hemoglobin polymerization. Recently, an oral anti-sickling agent, Voxelotor (GBT440), developed by Global Blood Therapeutics (GBT) has proved promising. Voxelotor prevents red cell sickling and inhibits the generation of HbS fibers that make red cells less flexible by blocking HbS intermolecular contacts [62]. In 2018, the FDA granted Breakthrough Therapy Designation (BTD) to voxelotor for the treatment of SCD and based on the results from a Phase ½ clinical study (NCT02285088), the FDA granted GBT with a new drug application in September of 2019. The published results demonstrated an increased hemoglobin levels, reduced hemolysis and hemoglobin aggregates in all patients who were treated for more than 28 days [63]. No severe adverse side effects were reported. A Phase 3 HOPE , double-blind, placebo-controlled study (NCT03036813) in SCD patients age 12 and older and a Phase 2A HOPE-KID 1 (NCT02850406) trial in pediatric patients with SCD aged 4 to 17 are currently ongoing.

1.5.4 Red Cell Transfusions

RBC transfusion therapy is considered a crucial treatment in decreasing morbidity and mortality in SCD. It is estimated that 90% of adults with SCD will receive at least one RBC transfusion for the treatment of acute or chronic complications associated with SCD [64]. These complications include perioperative, silent cerebral infarcts, acute anaemia, ACS, acute pain, and stroke. Following a RBC transfusion, there is an immediate reduction in the concentration of HbS-containing RBC and a correction of anaemia. The reduction in the concentration of HbS-containing RBC is likely to reduce the tendency for vaso-occlusion and vascular damage and the

correction of anaemia improves the oxygen carrying capacity which in turn changes the blood viscosity which can improve (or impair) oxygen delivery to tissues [65].

Unfortunately, RBC transfusions are linked to several adverse side effects and complications. Iron overload and alloimmunization are the most problematic complications associated with the transfusion [44], [64]–[68]. To combat iron overload, chelation therapy is implemented. There is a high rate of alloimmunization in patients with SCD due to alloantibodies and autoantibodies [67]. These can lead to delays in transfusion as well as increased labor and cost for RBC cross-matching. Additional complications may arise due to the increase in hematocrit levels and whole blood viscosity. Induced hyperviscosity from a large transfusion volume can inhibit oxygen delivery may promote vaso occlusion [69]. Thus, it is imperative to take extra care and precautions when determining exchange volumes. Furthermore, transfusions are less common in low income countries due to the cost, limited blood supply, increased risk of contamination, and infrastructure.

1.5.5 Curative Therapies

1.5.5.1 Stem Cell Transplantation

Ever since the discovery of SCD, researchers have been searching for a cure. In 1984, the first cure for SCD was accidentally discovered following a bone marrow transplant to treat a child's leukemia. Allogeneic hematopoietic stem cell transplants (HSCT) have since been successful as a curative treatment for SCD in 85-90% of patients [6]. However HSCT has limited administration due to a limited donor pool, cost, graft failure and the possibility of long-term adverse effects. Considering the low availability and risk of host rejection leading to morbidities and mortalities, HSCT is generally reserved only for the most severe cases of SCD, such as those

undergoing chronic transfusion therapy [6]. Patients with human leukocyte antigen (HLA)-matched sibling donors experience a mortality rate of 5% and an event free survival of approximately 90%. Unfortunately, only 10-20% of patients have an HLA sibling available and when an alternative donor is used, the mortality rate increases to 10-24% [44]. Furthermore, the high costs and required infrastructure seriously restrict HSCT treatment in lower income and developing countries [68], [70], [71].

1.5.5.2 Gene Therapies

Gene therapy is a promising potential treatment to abrogate SCD through the manipulation of HSC via a number of strategies including viral vector-mediated insertion of a function beta-globin gene, as well as gene-editing techniques with CRISPR/Cas9 that reduce intracellular sickling and enhance production of HbF [72], [73]. The major advantage of gene therapy over HSCT is the ability to use the patient's own stem cells thereby negating the need to identify a donor and eliminating associated complications and risks such as graft-versus-host disease. However, gene therapy like HSCT does require radiation exposure and chemotherapy. Phase ½ trials are currently underway to determine the efficacy and safety of gene therapy utilizing lentiviral vectors (NCT02247843, NCT02186418). These trials have estimated completion dates of August 2022 and June 2035. In addition, there are multiple phase ½ trials are currently recruiting patients to test the safety and efficacy of genome edited HSC through the use of various products including GPH101, EDIT-301, OTQ923 and HIX763 (NCT04819841, NCT04853576, NCT04443907).

1.6 Project Outline

1.6.1 Research Hypothesis

SCD is an inherited blood disorder that can manifest in a variety of symptoms and complications. The leading cause of death of individuals suffering with SCD are cardiopulmonary complications with approximately 30% of SCD deaths related to the heart. A better understanding of the mechanisms and pathways that contribute to the cardiomyopathies in SCD has the potential to uncover novel therapeutics to inhibit disease progression. The sickled vascular microenvironment is characterized as an inflammatory state.

This project proposes the use of an *in vitro* disease model to investigate the mechanisms that contribute to SCD-related cardiomyopathies. A pathological state will be induced by exposing cardiac tissues to ANG II or the sickled microenvironment, specifically, serum proteins. The sickled vascular microenvironment is characterized as an inflammatory state with increased ROS, that can lead to ischemia and endothelial dysfunction. The goal of this study is to recapitulate *in vivo* features of SCD-cardiomyopathies by investigating the effects of ANG II or the sickled serums on gene expression, and oxidative stress generation. This work will provide insight into the mechanisms and pathways that contribute to SCD related cardiomyopathies which has the potential to identify novel targets for treatments.

CHAPTER II

INDUCED CARDIAC DYSFUNCTION ON A CHIP

2.1 The Renin-Angiotensin-Aldosterone System and Cardiac Pathology

To create a landscape page, you just rotate the page using the "Orientation" option in the Layout Tab. This will put your page number at the bottom of the page. If you would like to print a hard copy and have the page number similar to the portrait pages, we can help you make those changes. The renin-angiotensin aldosterone system (RAAS) is a hormonal pathway involved in the homeostatic control of arterial pressure and extracellular volume. As indicated by the name, the three main components of the system are renin, angiotensin and aldosterone. The pathway begins with the biosynthesis of renin by juxtaglomerular cells (JGC). The JGC release mature renin from storage granules by an exocytic process. Since renin regulates the initial rate-limiting step of the RAAS, renin secretion acts as a key determinant of RAAS activity[74].

Renin secretion is regulated through interdependent factors including NaCl delivery to macula densa cells, negative feedback through direct action of angiotensin II (ANG II) on JGC, sympathetic nerve stimulation, and a renal baroreceptor mechanism. When renin is secreted, it acts upon circulating angiotensinogen (AGT) cleaving the 10 amino acids from the N-terminal to form the biologically inert decapeptide angiotensin I (ANG I) [75], [76]. In the human heart, chymase is responsible for the majority of ANG II generation from ANG I or the dodecapeptide ANG (1-12), as opposed to the use of angiotensin converting enzyme (ACE) as observed in the classical endocrine pathway [77]–[79]. ANG II is the vasoactive octapeptide (Asp-Arg-Val-Tyr-

Ile-His-Pro-Phe) that is considered the primary product of the RAAS, although other metabolites of ANG I and II may also play a significant role in biological activity [75], [76]. ANG II and the RAAS are key components in maintaining cardiovascular homeostasis in regard to hypertrophy, cardiac protection, arrhythmias, contractility, fibrosis and heart failure.

ANG II has two main receptors, the losartan-sensitive receptor termed AT1R and the losartan-insensitive receptor termed AT2R [80], [81]. Both AT1R and AT2R belong to the seven-transmembrane G protein-coupled receptor (GPCR) superfamily. The AT1R is expressed in various tissues including endothelium, heart, vascular smooth muscle, brain, kidney, adipose tissue, and adrenal gland and plays a central role in the physiological functions induced by ANG II [82], [83]. In addition, the cardiac pathogenesis, including inflammation, increased oxidative stress, hypertrophy, proliferation and extracellular matrix remodeling, induced by the molecular and cellular actions of ANG II are almost exclusively mediated by AT1R signaling mechanisms [82], [84], [85]. In contrast to AT1R, AT2R stimulation is associated with beneficial effects in the cardiovascular system through promotion of vasodilation, reduction of fibrosis, inflammation, and oxidative stress. Therefore, an appropriate balance between AT1R and AT2R activation and stimulation plays a crucial role in the regulation of physiological functions [86].

Dysregulation of the RAAS plays an integral role in the pathophysiology of cardiovascular disorders. *In vitro* and *in vivo* studies have reported that ANG II induces pathological conditions including myocardial infarction, hypertrophy, and heart failure [85], [87]–[93]. In cultured cardiomyocytes, ANG II has been shown to induce a series of changes indicative of a hypertrophic response including re-expression of fetal cardiac genes like natriuretic peptides, increase in cell size, and reorganization of contractile proteins [84], [85], [94]–[96]. Similarly, ANG II has been shown to induce endothelial dysfunction *in vitro* and *in*

vivo as demonstrated by reduced NO bioavailability, an increase in ROS, upregulation of adhesion molecules, and a proinflammatory state [85], [91], [97]–[100]. Furthermore, mice infused with ANG II led to cardiac hypertrophy fibrosis, increased blood pressure, and re-expression of fetal genes [85], [101]. To build upon these studies, I will exploit the pathological effects of ANG II to induce cardiac dysfunction *in vitro* using engineered neonatal ventricular mouse cardiomyocytes and mouse cardiac endothelial cells. *In vitro* disease models provide an affordable alternative to animal models. The work presented here on in will provide a better understanding of early stage cardiac dysfunction and disease progression.

2.2 Materials and Methods

2.2.1 Microcontact Printing

Engineered cardiac tissues were developed by seeding cardiac cells onto microcontact printed templates. The mask was previously constructed at Harvard University by Dr. Horton. Briefly, the mask was engineered using AutoCad (Autodesk, Inc., San Rafael, CA) to contain rectangular arrays of 15 μm lines with 2 μm spacings. Silicon wafers with SU-8 2002 photoresist (MicroChem, Newton, MA) coating were subjected to UV light. Subsequently, the wafers were exposed to SU-8 developer to expose the mask features. Afterwards, the wafers were subjected to salinization. Polydimethylsiloxane (PDMS) (Slygard 184, Dow Corning, Midland, MI) was poured onto the wafer to create stamps. The PDMS covered wafer was then degassed to remove all air bubbles before curing at 65°C for at least 4 hours. The cured PDMS stamps were carefully cut and removed from the wafer and cleaned in 70% ethanol. The PDMS stamps containing the rectangular arrays of 15 μm lines with 2 μm spacings were used to pattern fibronectin onto PDMS coated coverslips.

Figure 2.1 Visualization of PDMS Stamps using a light microscope PDMS Stamps with rectangular arrays of 15 µm lines with 2 µm spacings

This was accomplished by "inking" PDMS stamps was 50 µg/ml fibronectin (BD Biosciences, Bedford, MA) for 1 hour. The excess fibronectin was removed after 1 hour and the stamps were left to dry. While the stamps were drying, 15:1 (527:184) PDMS coverslips were cleaned and treated in a UVO cleaner for 8 minutes. Microcontact printing was then performed by gently placing the fibronectin coated side of the stamp onto a UVO treated coverslip. To ensure proper transfer, the stamp was lightly tapped. The stamp was then removed from the coverslip taking caution to avoid disruption of the pattern transfer onto the coverslip. The coverslips were then background treated with 2.5 µg/ml fibronectin for 10 minutes and subsequently rinsed three times with PBS. The coverslips were stored submerged in PBS at 4°C until cell seeding.

2.2.2 Cell Culture

Cell culture reagents were purchased from Cell Biologics (Chicago, IL) unless otherwise specified. Mouse primary cardiac endothelial cells (MCEC) were cultured in Endothelial Cell Medium supplemented with 5-10% fetal bovine serum (FBS), 1% antibiotic-antimycotic, 0.1% epidermal growth factor, 0.1% Heparin, 0.1% hydrocortisone, 0.1% vascular endothelial growth

factor, 0.1% endothelial cell growth supplement, and 2mM L-Glutamine. Cells were seeded into a T-25 flask precoated with 0.1% gelatin until confluent. Cell culture was carried out at 37□C in a humidified atmosphere containing 5% CO_2. Once confluent the cells were dissociated using 2ml of 0.25% trypsin-EDTA solution and passaged into T-75 flask precoated with 0.1% gelatin. The cell culture media was changed every other day. Once confluent, cells were seeded onto chips at a density of 300,000 cells/cm^2. On the following day, the cell culture media was supplemented with either 0.25% BSA (Sigma Aldrich, St. Louis, MO) or 2% AA/AS/SS serum rather than FBS for the remainder of the experiment. For the ANG II experiments, the tissues were exposed to 5 nM, 100 nM or 1 □M of ANG II daily. In the serum experiments, the media was changed every other day.

2.2.3 Cell Harvest

Transgenic sickle cell mice have been utilized to better understand the complex mechanisms and pathways that are associated with the pathophysiology of SCD. There are two common mice models for SCD: Berkley and Townes. The Berkley mice model knocks-out genes for endogenous mouse α and β globins (α-/-, β-/-) with transgenes for the expression of human α, β^s, Aγ, $^G\gamma$, and β globins [102]. As a result, Berkley mice express HbS almost exclusively. In comparison, the Townes mice model knocks-in genes replacing the endogenous mouse α-globin genes with human α-globin genes and endogenous mouse β globin genes with human Aγ and β^s globin genes [103]. One of the major differences between these mice models pertains to the transition from fetal hemoglobin (γ-globin) expression to sickle β-globin expression. In the Berkley mice the transition is complete by 15 days gestation. This leads to increased perinatal lethality translating into small litter sizes [104]. This constitutes a major limitation when

employing the Berkley mice model. In contrast, the Townes mice transition is complete at 1 month of age thereby mimicking the timeline found in humans. For these reasons, we chose to employ the Townes mice model.

All animal procedures and the experimental protocols were approved by the Mississippi State University Animal Care and Use Committee. All materials were purchased from Thermo Scientific (Waltham, MA) unless otherwise stated. Breeding pairs were ordered from Jackson Laboratories (Stock No: 013071, Townes model, hα/hα::, β^A/β^s, hα/hα::383 γ-β^A/-1400 γ-β^S). Mice were bred and phenotyped for control (HbAA), sickle trait (HbAS), and sickle cell anemia (HbSS) human hemoglobins. A previously published cardiomyocyte harvest protocol was modified and used for this study[105]–[107]. Briefly, ventricles from two-day-old mice were harvested, rinsed with Hanks Balanced Salt Solution (Gibco Cat# 14175-079), and enzymatically digested using trypsin (1mg/ml) for 12 hr at 4°C. Tissues were then mechanically dissociated three times in collagenase II (1mg/ml, Worthington Biochemical, Lakewood, NJ). To reduce the fibroblast population, the cell suspension was incubated in T-25 flasks containing M199 media supplemented with 10% Heat inactivated FBS (Gibco Cat. #16140-071), 2 mM L-glutamine (Gibco Cat. #25030-081), 0.1 mM nonessential amino acids (Gibco Cat. #11140-050), 10 μM HEPES (Gibco Cat. #15630-080), 19.4 μM glucose (Sigma Aldrich, St. Louis, MO), 50 U/mL of penicillin (Sigma Aldrich, Cat. #P-4687), and 1.5 μM B12 (Sigma Aldrich, Cat. #V-2876) for 45 minutes at 37°C. The cell suspension was collected and counted. Cells were then seeded onto chips at a density of 300,000 cells/cm^2. After 24 hours, a dead cell wash-off was performed using PBS and the media was changed. On the following day, the cell culture media was supplemented with either 0.25% BSA (Sigma Aldrich, St. Louis, MO) or 2% AA/AS/SS serum rather than FBS for the remainder of the experiment. For the ANG II experiments the media was changed and the

tissues were exposed to 5 nM, 100 nM or 1 □M of ANG II daily. In the serum experiments, the media was changed every other day.

2.2.4 Gene Expression

Cell lysates were collected at 24 h, 72 h, and 1 week after initial ANG II or serum dosing. RNA was extracted using the Zymo Quick-RNA MiniPrep kit (Zymo, Irvine, CA). The Nanodrop spectrophotometer (Thermo Scientific, Waltham, MA) was used to determine the concentration of RNA. First strand complementary DNA (cDNA) synthesis was then performed using SuperScript III (Invitrogen, Carlsbad, CA). Quantitative real-time polymerase chain reaction (qRT-PCR) was then conducted using the QuantStudio 3 Real-Time PCR System (Thermo Scientific, Waltham, MA). Each sample was tested in duplicate on each plate for each experiment. Primer information can be found below in Table 2.1.

Table 2.1 PCR Primer gene list for ANG II and sickled microenvironment studies

Symbol	Name	Accession	Forward (5'-3')	Reverse (5'-3')
RPL13a	Ribosomal Protein L13a	BC086896	ATGACAAGAAAAAGCGGATG	CTTTTCTGCCTGTTTCCGTA
Gusb	Glucuronid	NM_0103	AATGAGCCTTCCTCTG	AACTGGCTATTCAGC
IL6	interleukin 6	NM_0311	CTACCCCAATTTCCAA	ACCACAGTGAGGAAT
CTGF	connective tissue	NM_010217	GTAACCGGGGAGGGAAATTA	TACTTGCCACAAGCTGTCCA
NPPB	natriuretic peptide type B	NM_008726	CAGCTCTTGAAGGACCAAGG	AGACCCAGGCAGAGTCAGAA

Table 2.1 (continued)

Symbol	Name	Accession	Forward (5'-3')	Reverse (5'-3')
NR4A	nuclear receptor subfamily	NM_010444	CTGGACGTTATCCGAAAGTG	GTCAATCCAATCACCAAAGC
ICAM	intercellular adhesion	NM_010493	CCTGCCTAAGGAAGACATGA	CCCAGACTCTCACAGCATCT
HAMP	hepcidin antimicrobia	NM_032541	CCAATGCAGAAGAGAAGGAA	GGGAGGGCAGGAATAAATAA

2.2.5 Kinetic Oxidative Stress

CellRox Green Reagent (Thermo Fischer Scientific, Waltham, MA) was used to quantify the formation of reactive oxygen species (ROS) *in vitro*. The dye is weakly fluorescent while in a reduced state. Once the dye is oxidized by ROS it binds to DNA and thus primarily localized in the nucleus and mitochondria. MCEC were seeded at a density of 250,000 cells per ml in a 96- well plate precoated with 15:1 PDMS. For the ANG II experiments, the cells were cultured in media supplemented with 0.25% BSA. For the serum experiments, the cells were cultured in media supplemented with 2% FBS until their respective treatment time. The cells were treated for 1 week, 72 hr, 24 hr and 1 hr with either ANG II (5 nM, 100nM or 1□M) or 2% AA, 2% AS, or 2% SS serum. After one week, 5□M CellRox Green reagent was added to each sample incubated for 30 minutes. Cells were then washed three times with 1X PBS. Afterwards, 150□l of cell media was added to each well. Fluorescent intensity (485/520 nm) was analyzed using Cytation 5 (BioTek, Winooski, VT) every 10 minutes for two hours at 37□C and 5% CO_2.

2.2.6 Data Handling

2.2.6.1 Data Handling for Oxidative Stress Experiments

Prior to performing statistical analysis on the oxidative stress experiments the raw data was transformed. All of the replicate wells from each individual plate were first averaged together. Next, the averaged blank wells were subtracted from the averaged experimental wells on each plate. Finally, the data was normalized from zero to one on a plate basis. The minimum value on each individual plate was represented as a zero and the maximum value on each plate was represented as a one. The transformed data was then statistically analyzed as described below.

2.2.6.2 Data Handling for Gene Expression Experiments

Prior to performing analysis on the gene expression experiments the raw data was automatically transformed using the QuantStudio Design and Analysis Software. The cycle threshold (C_T) analysis was performed during the PCR stage as well as the melt curve stage. An amplification value of less than 0.1 was automatically flagged as no amplification via the software. Primers that failed to amplify on all plates were excluded from further analysis. The relative minimum and maximum quantification were determined using a 95% confidence level. The relative fold change was determined using the $\Delta\Delta$ C_t method through the QuantStudio Design and Analysis Software using the specified endogenous control primers RPL13A or GUSB [108]. For ANG II studies, gene expression was normalized to untreated tissues at the respective time point. In MCEC serum treated studies, gene expression was normalized to 2% AA serum treated tissues at the respective time point. In Cardiomyocyte treated studies, gene expression was normalized to the AA cardiomyocytes treated with 2% AA serum or 0.25% BSA,

at the respective time point. Then a pivot table was utilized to aggregate the data using the mean relative quantification (RQ) for each sample and gene. Any inconclusive values were omitted from the aggregation step. This was then used to generate a heat map using MatPlotLib. If the RQ was 1 the box was shaded green and if the RQ was below 1 the box was shaded red to represent upregulation and downregulation, respectively.

2.2.7 Statistical Analysis for Oxidative Stress Experiments

After completion of data transformation, statistical analysis was performed. I had no reason to believe the relationship was nonlinear and thus a multiple regression model was used to interpret the results, find trends, and statistical significance. To analyze the data, Python 3 was employed. Python data analysis library, PANDAS, was used to load and organize the transformed data. Then python's statsmodel library was used to perform multiple regression analysis. The multiple regression analysis was used to determine the strength of the relationship between concentration, duration, or serum type to the amount of oxidative stress produced. To quantify the effect of the HbS, the number of S alleles present in the serum was used to categorize the data as follows: AA=0, AS=1, and SS=2.

2.3 Results

2.3.1 ANG II Oxidative Stress

I found two important trends in the ANG II treatments for the MCEC and CM oxidative stress analysis. In the MCEC experiments, the concentration of ANG II demonstrated a negative correlation -4.5*10-5 nM^-1 with a p-value of 0.045. This indicates that less oxidative stress was

produced with an increased concentrated of ANG II. A visual representation of this analysis can be seen in the figures below. The duration of the experiment in MCEC had a positive correlation of 0.003 per hour and a p-value of 0.073. This suggest the longer the experiment continued the higher the concentration of oxidative stress produced in all wells as represented by an increased relative fluorescence.

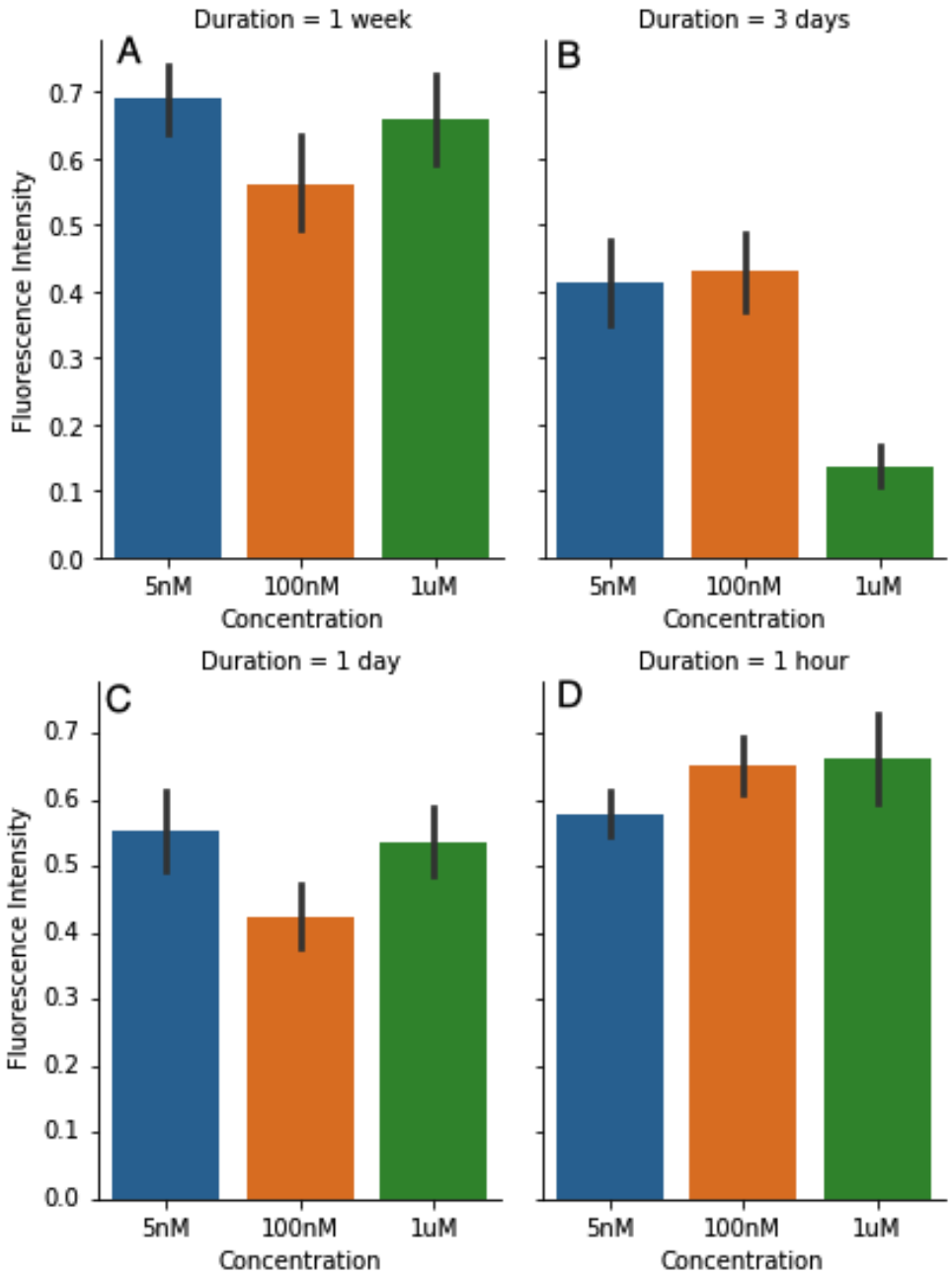

Figure 2.2 The effect of ANG II exposure on oxidative stress in MCEC

Fluorescence intensity measured in MCEC treated with ANG II in media supplemented with 0.25% BSA. The tissues were exposed to varying concentrations of ANG II. A. The effect of ANG II after 1 week of exposure. B. The effect of ANG II after 3 days of exposure. C the effect of ANG II after 1 day of exposure. D. The effect of ANG II after 1 hr of exposure. (Mean ± SEM, N=3 tissues)

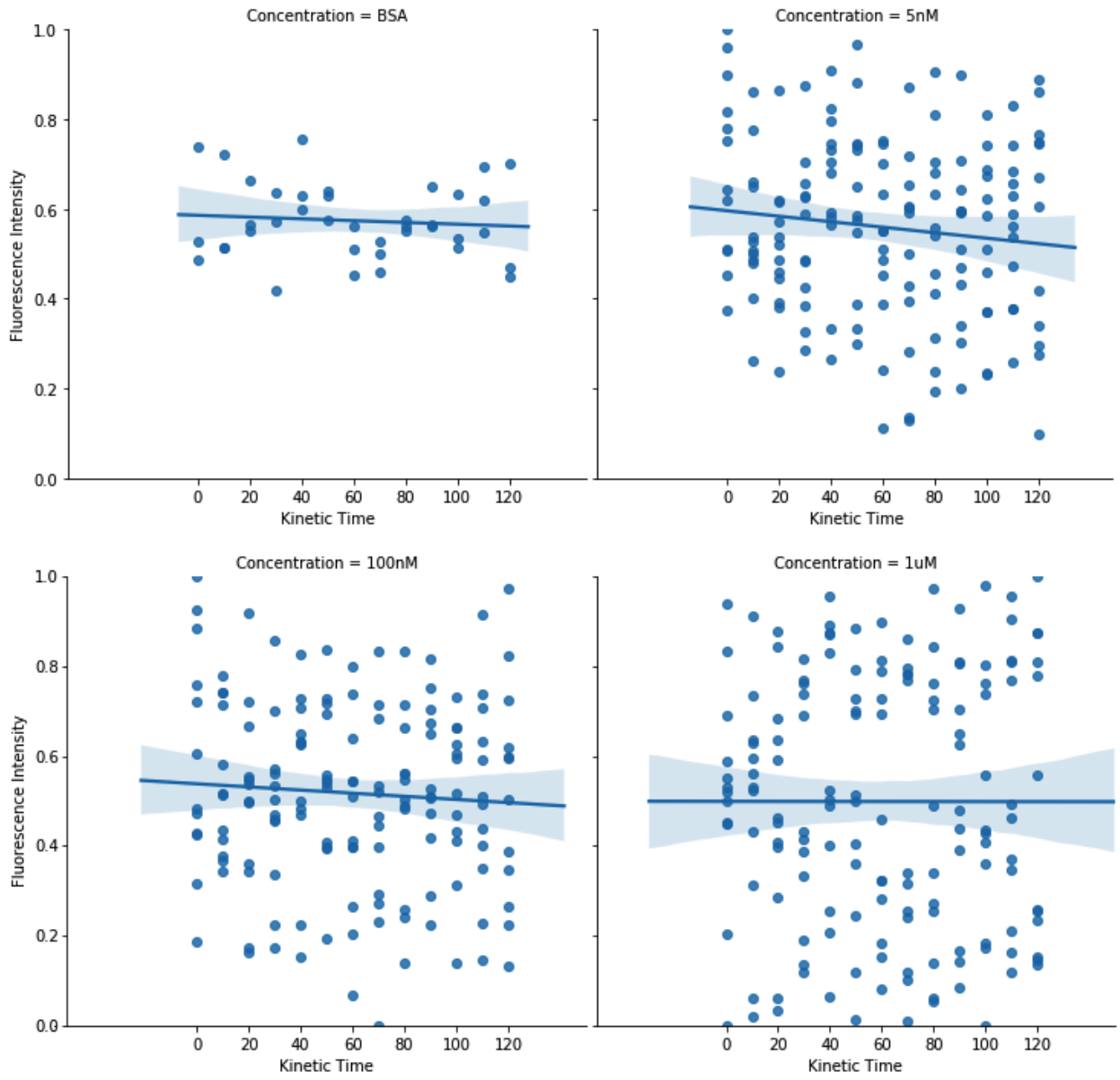

Figure 2.3 The effect of ANG II exposure on the kinetic oxidative stress in MCEC

Fluorescence intensity in MCEC over the course of the 2-hour kinetic read. Tissues were treated with varying concentrations and durations of of ANG II prior to conducting the kinetic read. No significant differences or trends in the fluorescence intensity were detected in the kinetic read.

In the CM oxidative stress analysis, the concentration of ANG II produced a negative correlation coefficient of -2*10^-4 nM^-1 with a p-value of less than 0.0001. This indicates an inverse relationship between the concentration of ANG II used and the oxidative stress produced.

In contrast to the MCEC oxidative stress experiments, the duration of the experiment was negatively correlated with a correlation coefficient of -3.5*10^-5 per hour and a p-value of 0.6. I then asked whether the CM cell type had an effect on the oxidative stress produced during the ANG II dosing. I discovered the CM cell type had a positive correlation of 0.037 per number of S alleles with the SS CM exhibiting the highest oxidative stress with a p-value of less than 1*10^-4.

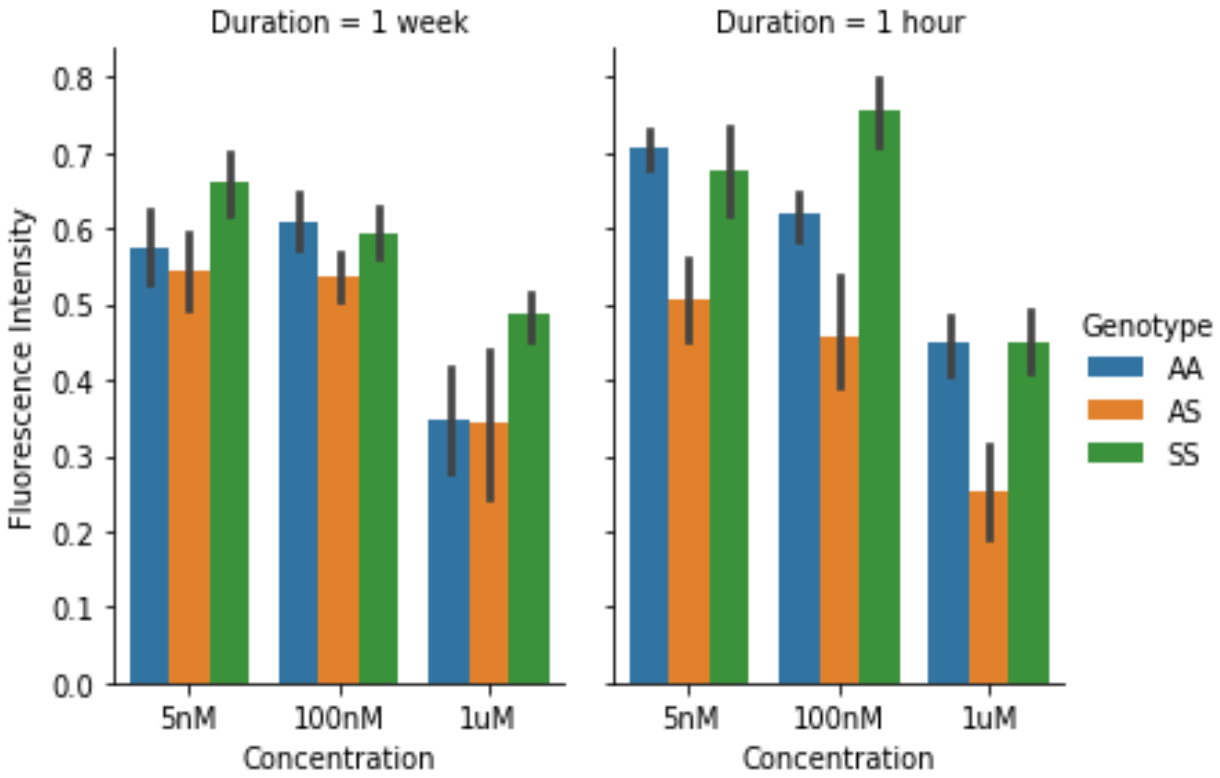

Figure 2.4 The effect of ANG II exposure on cardiomyocyte oxidative stress

Fluorescence intensity measured in Townes AA, AS, SS neonatal cardiomyocytes treated with ANG II in media supplemented with 0.25% BSA. The tissues were exposed to varying concentrations of ANG II. (Mean ± SEM, N=2 tissues)

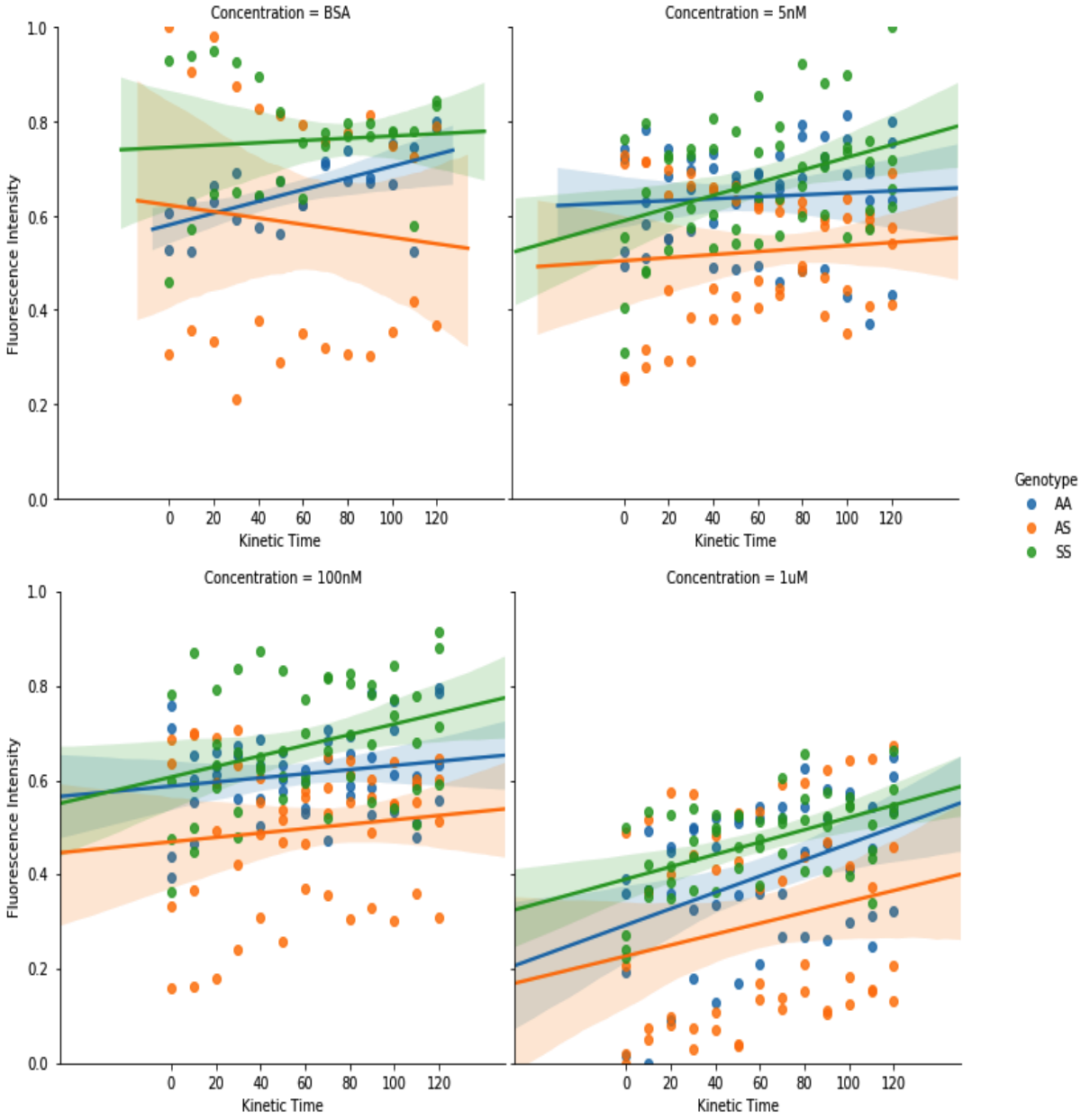

Figure 2.5 The effect of ANG II exposure on the kinetic oxidative stress in cardiomyocytes

Fluorescence intensity measurd over a 2-hour kinetic read in Townes AA, AS, SS neonatal cardiomyocytes after exposure to varying concentrations of ANG II

2.3.2 Serum Oxidative Stress

I found two important trends in the serum dosing for the MCEC and CM oxidative stress analysis. In the MCEC experiments, the number of S alleles present in the serum was positively correlated with a correlation coefficient of 234 per S allele and a p-value of less than .0001. Similarly, to the ANG II treatments, the duration of the experiment in MCEC had a positive correlation of 0.1276 per hour with a p-value of 0.04. This suggests the longer the experiment continued the higher the concentration of oxidative stress produced.

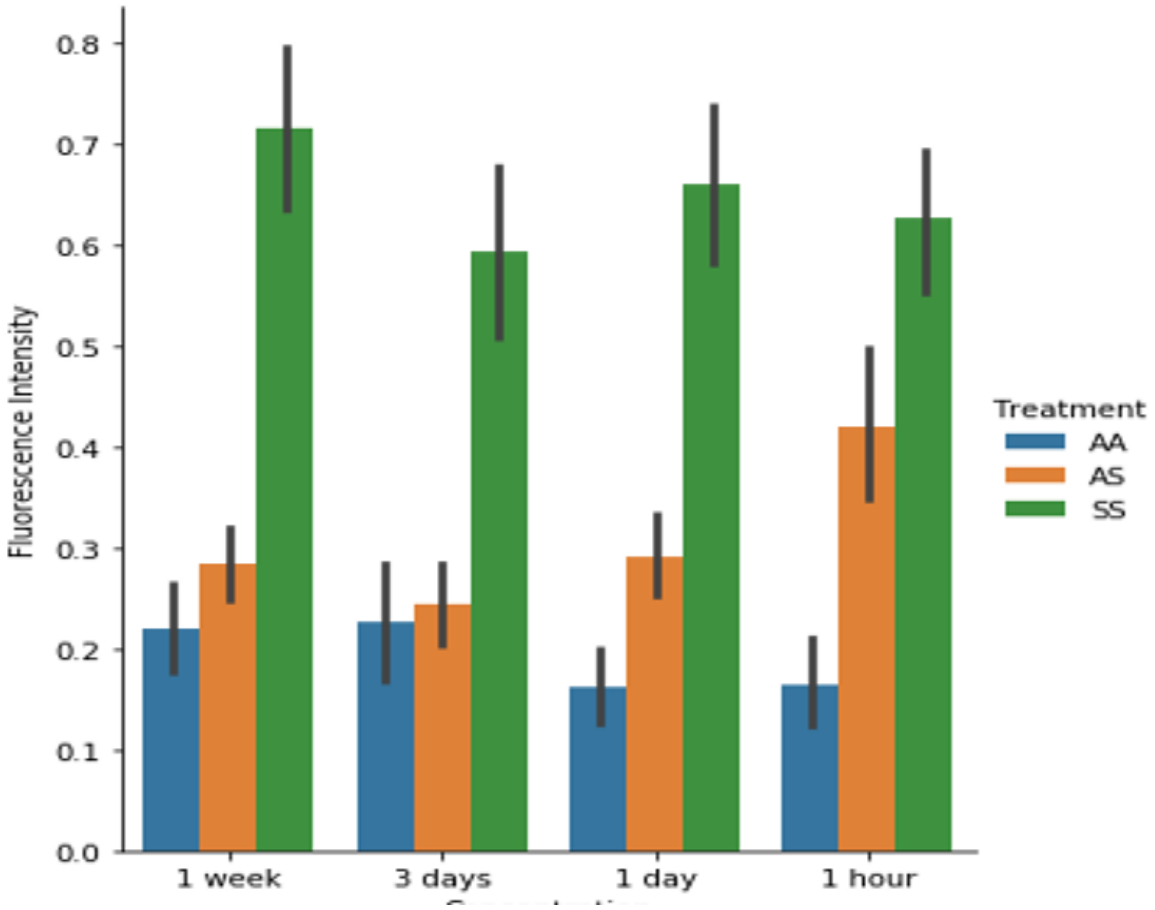

Figure 2.6 The effect of the sickled microenvironment on MCEC oxidative stress

CellRox fluorescence intensity of MCEC after exposure to 2% serum derived from Townes AA, AS, SS genotypes. For the serum experiments, the cells were cultured in media supplemented with 2% FBS until their respective treatment time. (Mean ± SEM, N=3 tissues)

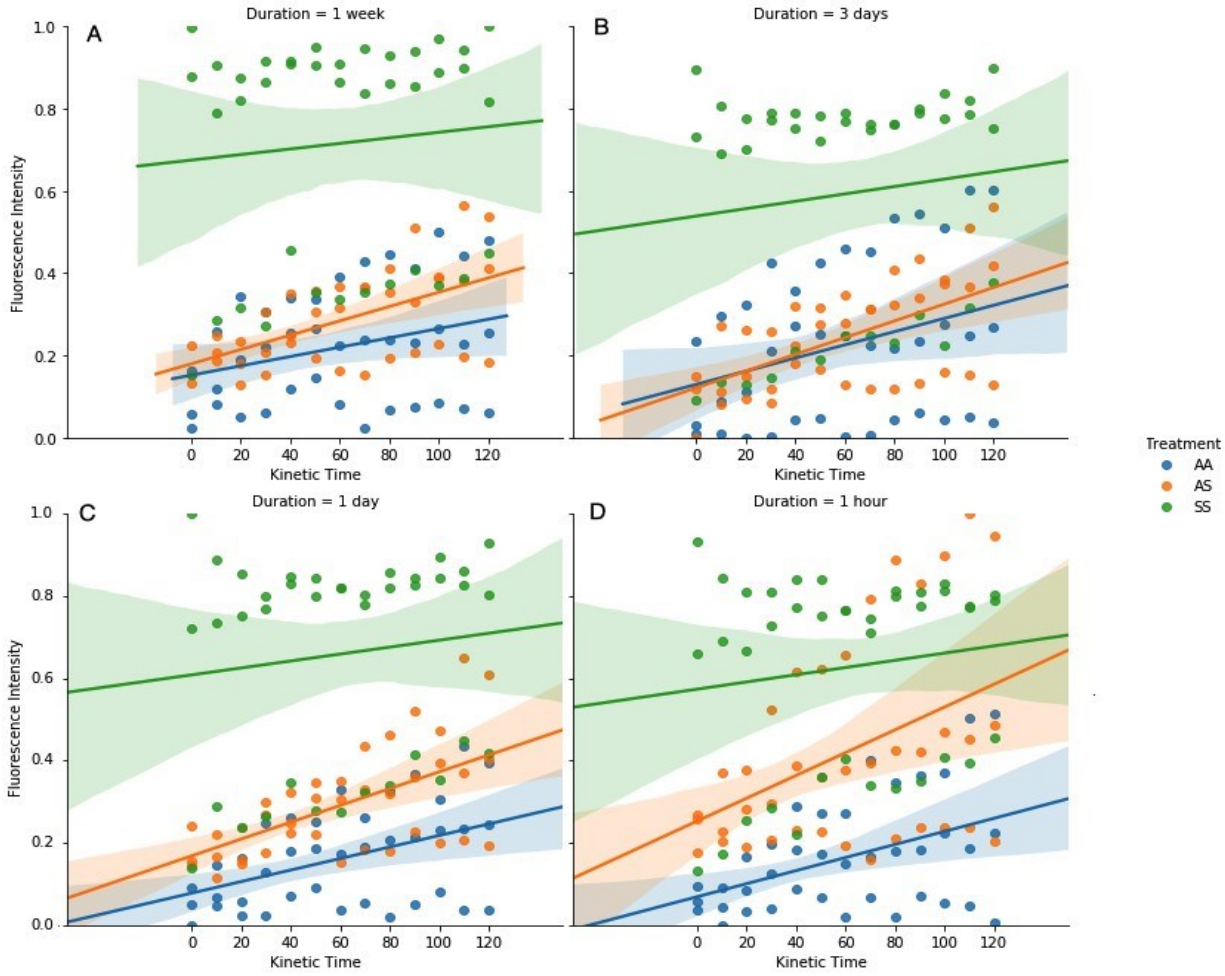

Figure 2.7 The effect of the sickled microenvironment on MCEC kinetic oxidative stress

CellRox fluorescence versus kinetic time in MCEC following exposure to 2% serum derived from Townes AA, AS, SS genotypes. N=3. For the serum experiments, the cells were cultured in media supplemented with 2% FBS until their respective treatment time. A. Experimental exposure for 1 week prior to kinetic plate read. B. Experimental exposure for 3 days prior to kinetic plate read. C. Experimental Exposure for 1 day prior to kinetic plate read. D. Experimental exposure for 1 hour prior to kinetic plate read. There was a general trend of increased fluorescence intensity over the kinetic read.

In the CM oxidative stress analysis, I observed a similar trend as seen in the MCEC. The number of S alleles present in the serum was positively correlated with a correlation coefficient of 32.53 per S allele and a p-value of 0.34. In contrast to the MCEC, the duration of the experiment produced a negative correlation coefficient of -0.37 per hour with a p-value of 0.26. Next I asked whether the CM cell type had an effect on the oxidative stress produced during the serum dosing. The analysis revealed a negative correlation between the amount of oxidative stress produced and the number of S alleles present with a correlation coefficient of -91 and a p-value of less than 0.0001.

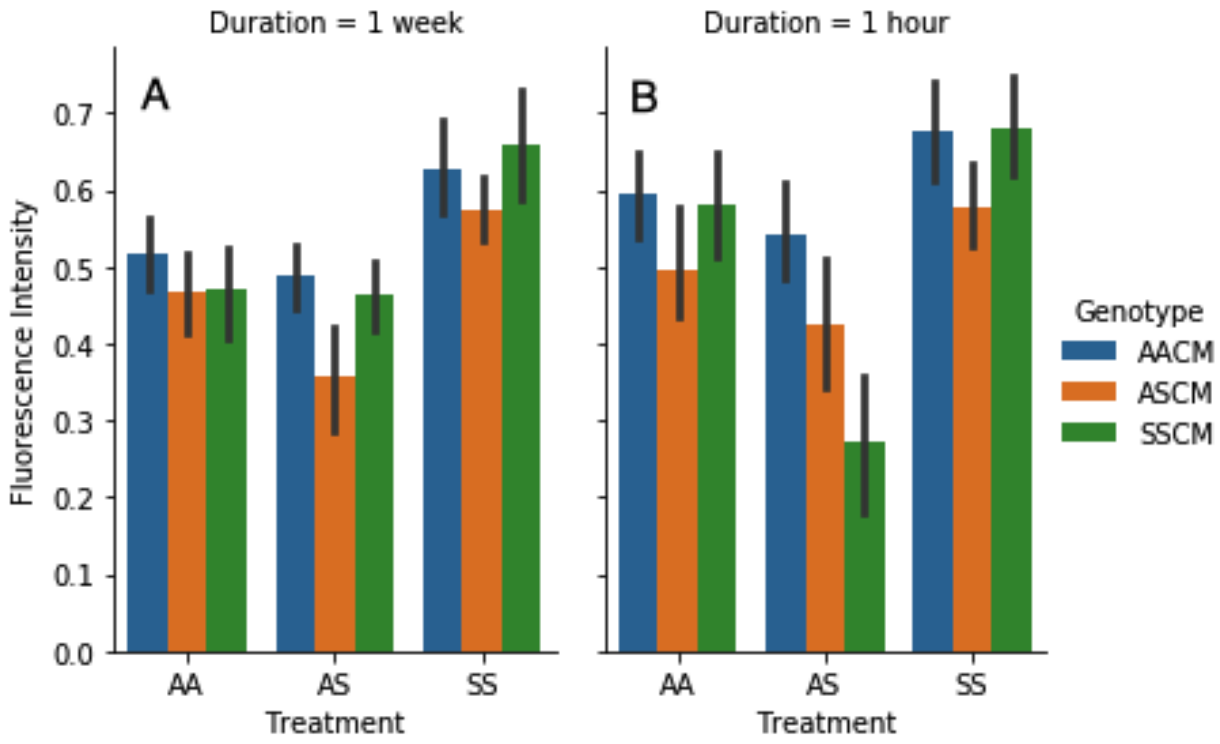

Figure 2.8 The effect of the sickled microenvironment on cardiomyocyte oxidative stress

The fluorescence intensity was measured in Townes neonatal cardiomyocytes, AA, AS, and SSgenotypes. A. The cardiomyocytes were cultured in media supplemented with 2% serum derived from Townes AA, AS, or SS genotypes for 1 week. B. The cardiomyocytes were cultured in media supplemented with 2% serum derived from Townes AA, AS, or SS genotypes for 1 hr prior. (Mean ± SEM, N=2 tissues)

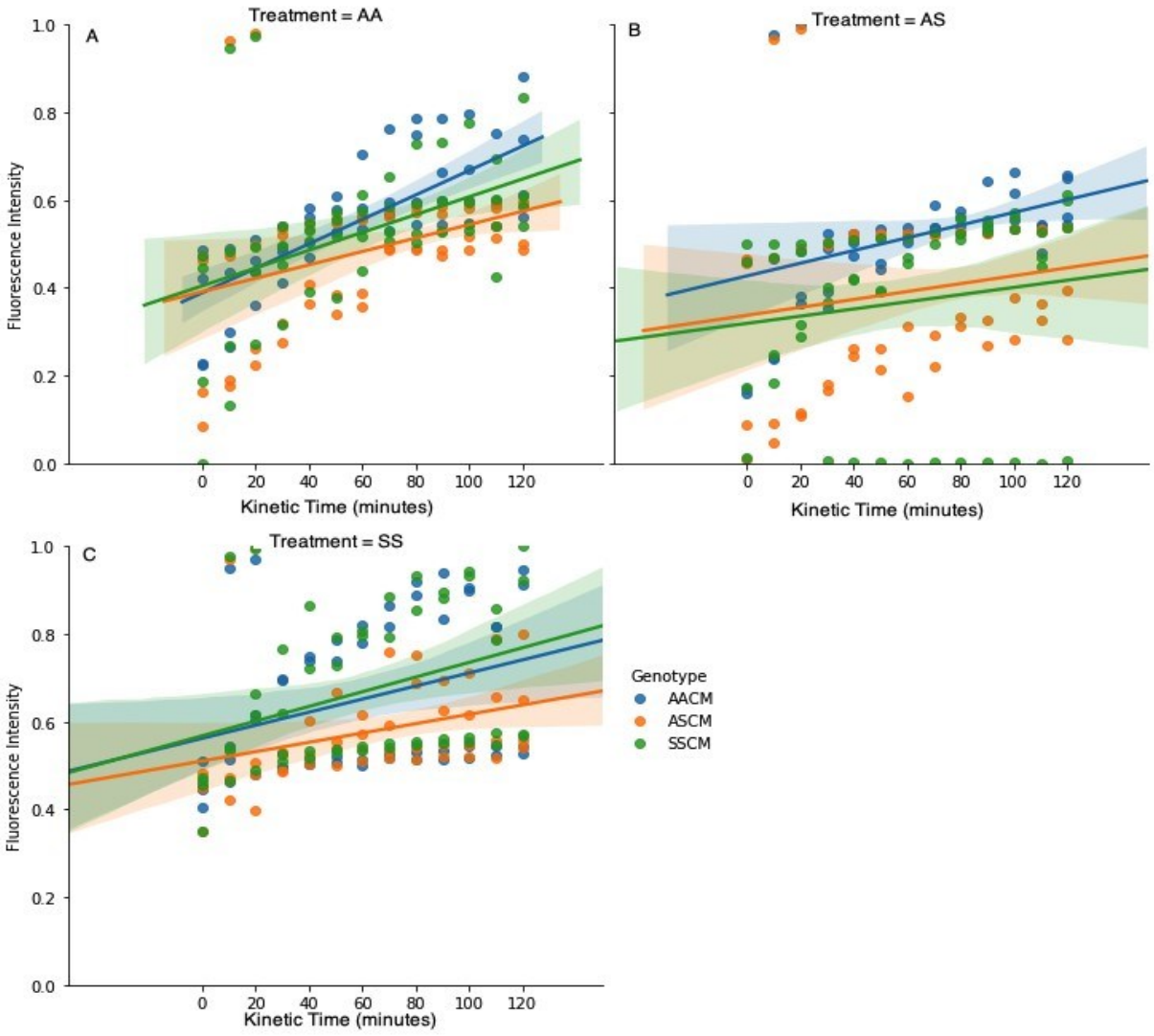

Figure 2.9 The effect of the sickled microenvironment on cardiomyocytes kinetic oxidative stress

CellRox fluorescence versus kinetic time measured in Townes neonatal cardiomyocytes, AA, AS, and SS genotypes. A. AA, AS and SS cardiomyocytes cultured in media supplemented with 2% AA serum. B. AA, AS and SS cardiomyocytes cultured in media supplemented with 2% AS serum. C. AA, AS and SS cardiomyocytes cultured in media supplemented with 2% SS serum. There was a general trend of increased fluorescence intensity over the kinetic read.

2.3.3 Gene Expression

I performed qRT-PCR to examine the gene expression profile of genes known to be influenced by hypertrophy and/or heart failure. The MatPlotLib was then used to generate a color-coded mosaic to present a visual representation of relative fold regulation in treated tissues. In MCEC, the heatmap revealed the greatest differences in gene expression occurred 24 hr after initial 5nM ANG II treatment. The analysis displayed an upregulation of interleukin (IL)-6, connective tissue growth factor (CTGF), natriuretic peptide B (Nppb), nuclear receptor transcription factor (NR4A), and intercellular adhesion molecule (ICAM). These genes have been shown to be upregulated in hypertrophy and heart failure in *in vitro* and *in vivo* studies [85], [90], [96], [109]–[112]. These results indicate that 5nM ANG II induced a pathological gene expression profile in our cardiac engineered tissues after 24 hours.

Figure 2.10 ANG II induces pathological gene expression profile in MCEC

Heatmaps were created from qRT-PCR array relative quantification data over the duration of the experiment. The quantification was normalized to the control tissues at the respective time point. RPL13a was used as the housekeeping gene. Gene expression profiles differed the most from the control after 24 hours of 5nM ANG II exposure. Upregulation is indicated by shades of green and downregulation is indicated by shades of red.

In ventricular cardiomyocytes, the analysis revealed the greatest differences in gene expression following 1μM ANG II treatment. The AACM displayed upregulation in IL-6, CTGF, Nppb, and hepcidin (HAMP). Using the untreated AACM as the control tissues, the SSCM displayed an upregulation in IL-6 and CTGF after exposure to 1μM ANG II for 1 week. These results indicate that we were able to induce a pathological gene expression profile in our healthy CM using ANG II.

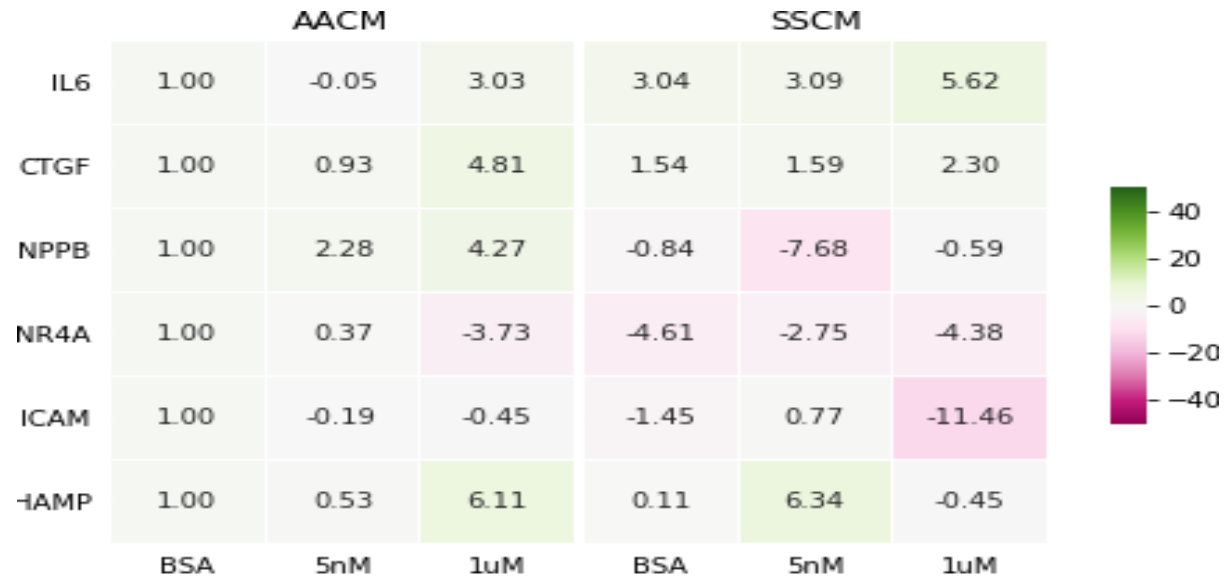

Figure 2.11 ANG II induces pathological gene expression profiles in cardiomyocytes

Heatmaps were created from qRT-PCR array relative quantification data over the duration of the experiment. The quantification was normalized to the AA CM control tissues at the respective time point. RPL13a was used as the housekeeping gene. Gene expression profiles differed the most from the control after 1 week of 1μM ANG II exposure. Upregulation is indicated by shades of green and downregulation is indicated by shades of red.

To examine the direct effects of the sickled microenvironment, specifically serum proteins, on cardiomyocyte health, I treated MCEC and CM with 2% AA, AS, or SS serum. In the MCEC, relative fold regulation and fold change was normalized to 2% AA treated tissues at the respective time point. In the CM, relative fold regulation and fold change was normalized to AACM treated with 2% AA at the respective time point. In the MCEC, the analysis revealed an upregulation in IL-6 and NR4A and downregulation in CTGF, Nppb, ICAM, and HAMP, 1 week after initial 2% SS serum exposure. In the AA CM, the analysis revealed an upregulation in CTGF and a downregulation in IL-6, Nppb, NR4A, ICAM and HAMP, 1 week after initial 2% SS serum exposure. For comparison, the SS CM displayed downregulation in IL-6, CTGF, Nppb, NR4A, ICAM and HAMP, 1 week after initial 2% SS serum exposure.

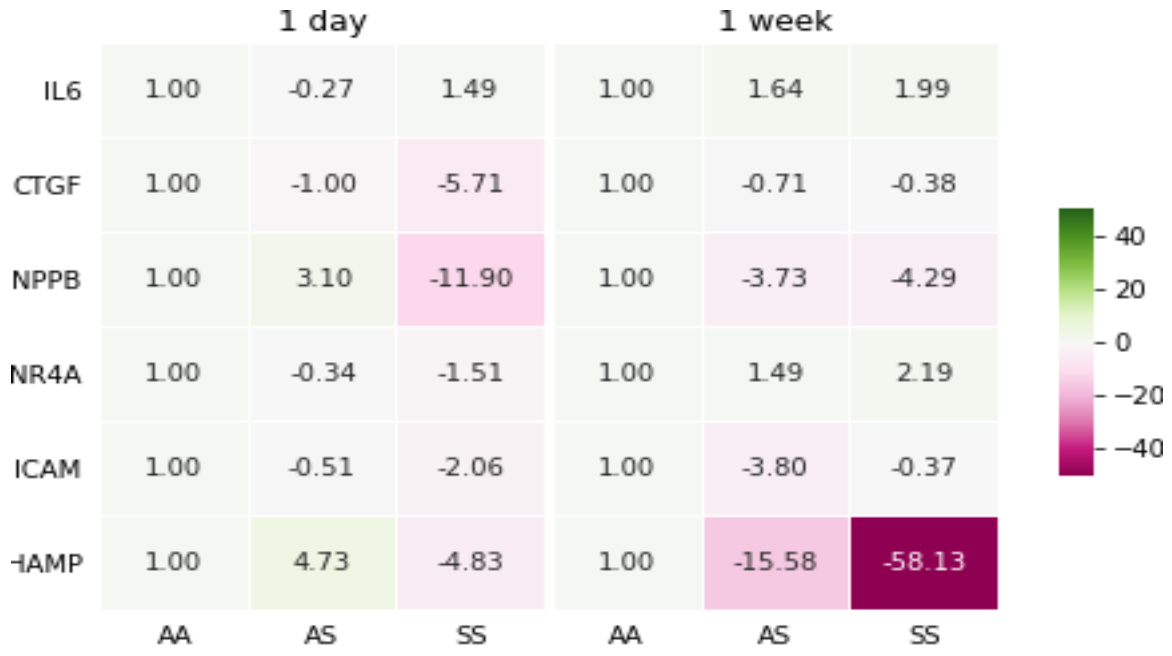

Figure 2.12 The effect of the sickled microenvironment on gene expression profiles in MCEC

Heatmaps were created from qRT-PCR array relative quantification data over the duration of the experiment. The quantification was normalized to the 2% AA control tissues at the respective time point. RPL13a was used as the housekeeping gene. Upregulation is indicated by shades of green and downregulation is indicated by shades of red.

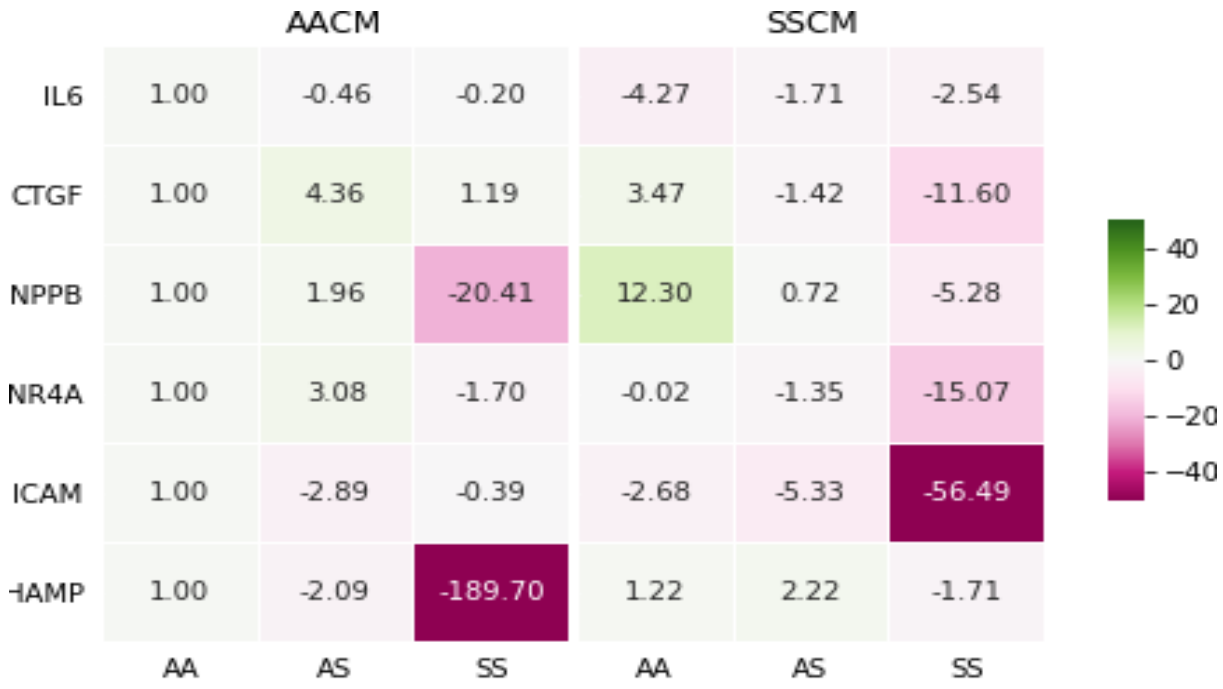

Figure 2.13 The effect of the sickled microenvironment on gene expression profiles in cardiomyocytes

Heatmaps were created from qRT-PCR array relative quantification data over the duration of the experiment. The quantification was normalized to the AA cardiomyocytes treated with 2% AA serum at the respective time point. RPL13a was used as the housekeeping gene. Upregulation is indicated by shades of green and downregulation is indicated by shades of red.

2.4 Discussion

In this study, I simulated ANG II induced cardiac failure and studied the effects of the sickle microenvironment on a chip using engineered mouse cardiac tissues. Gene expression profiles in the ANG II treated tissues indicated a pathological state with upregulation in biomarkers for inflammation, cell adhesion, wall stress and ECM related genes [85], [90], [109], [110]. This is consistent with previous *in vitro* and *in vivo* studies implicating ANG II as a major

contributing factor in the pathogenesis of cardiovascular diseases and heart failure. Gene expression analysis is commonly used to characterize disease states, define early diagnosis and is utilized to establish potential therapeutic targets. I observed an increase in interleukin (IL)-6, connective tissue growth factor (CTGF), natriuretic peptide B (Nppb), nuclear receptor transcription factor (NR4A), and intercellular adhesion molecule (ICAM) gene expression. It has been previously established that inflammatory cytokines, including IL-6, play crucial roles in early and late stages of cardiac remodeling and heart failure [110], [113]–[115]. In isolated cardiomyocytes, IL-6 causes negative inotropic effects. Additionally, endothelium derived IL-6 is believed to be involved in adaptive hypertrophic responses [111]. Furthermore, inhibition of IL-6 in a mice model lead to a decrease in cardiomyocyte hypertrophy and cardiac fibrosis, demonstrating the pro-hypertrophic and pro-fibrotic properties of IL-6 [111]. Studies have also indicated that CTGF plays a role in hypertrophy and cardiac fibrosis [116]–[118]. CTGF is a secreted protein that plays an essential role in ECM synthesis. It is believed that CTGF signaling pathway is an important mechanism involved in the development of diastolic heart failure.

Natriuretic peptides are commonly synthesized in the atria and left ventricle in response to elevated wall stress. As a result, they are commonly used as diagnostic and prognostic markers for hypertrophy and heart failure [119]. Elevation of NR4A has been observed in ECs as part of proinflammatory response and in CMs after ischemia/reperfusion injury [120]. Furthermore, NR4A has been implicated as a critical negative regulator of ANG II induced vascular remodeling in cardiovascular diseases [121].

All of the aforementioned genes have been correlated with ANG II induced cardiac hypertrophy, fibrosis and/or heart failure. Interestingly, exposure to the sickled microenvironment led to a downregulation in the majority of these genes suggesting the

cardiomyopathy observed in SCD occurs via a different mechanism of action or requires longer exposure. Additional testing incorporating a larger microarray or prolonged culture would shed some light on the progression of cardiomyopathy in SCD.

In addition, ANG II has been reported to increase ROS generation, specifically by stimulating NADPH to produce superoxide and hydrogen peroxide (H_2O_2) [85], [93]. The results of the oxidative stress experiments displayed a negative correlation between ANG II concentration and ROS generation. These results appear to be contradictory to what was expected; however, previous users have reported that H_2O_2 quenched CellRox's fluorescence [122], [123]. This interaction could explain why a negative correlation between ANG II concentration and fluorescence intensity was observed. In comparison, when the tissues were exposed to a sickled microenvironment, specifically serum proteins, an increase in ROS generation was observed. This is indicative of an inflamed state as is expected in the pathogenesis of cardiovascular disease [124]. It should be noted that the CellRox reagent only detects intracellular ROS and does not capture intercellular ROS. Further testing and analysis are required to quantify the intracellular and intercellular ROS generation.

In vitro disease models using organs-on-chip platforms can serve as diagnostic tools for therapeutic applications. This study utilized PDMS in conjunction with ECM proteins to employ a biologically relevant platform. PDMS is commonly used to fabricate *in vitro* platforms due to its biocompatibility, gas permeability, and optical clarity. To overcome the hydrophobic nature of PDMS, surface treatment is required to induce a hydrophilic surface to facilitate cell and protein adhesion. A fibronectin coating was incorporated because it is a major constituent of cardiac ECM [125]. The endothelial cell monolayers combined with a protein coating serves as a model endothelium. The work presented here indicates that I was able to recapitulate

pathological genetic profiles indicative of cardiac pathophysiology in cardiomyocytes and endothelial cells. We plan on building upon our results by constructing a co-culture device consisting of engineered cardiac tissues composed of cardiomyocytes as well as endothelial cells.

CHAPTER III

CONCLUSION AND FUTURE WORKS

3.1 Conclusion

This study focused on two of the essential cell lines that are responsible for the heart's structure and signaling cascades as a preliminary step for the development of a microfluidic system for examining cardiovascular diseases like SCD. To provide a better understanding of the complex cell-cell interactions in the development of cardiac dysfunction we needed to first investigate the individual cell response. I found that ANG II induced gene expression profiles indicative of cardiac pathophysiology. When the cardiac tissues were exposed to the sickle microenvironment and increase in oxidative stress was observed. This signifies that a sickle microenvironment is one of an inflamed state. However, the results of the ANG II oxidative stress experiments were contradictory to what was expected with a decrease in ROS generation. This could be attributed to limitations of the reagents used and will require further testing and analysis to confirm. The genetic profiles observed are similar to reported ANG II effects and are known biomarkers for hypertrophic cardiomyopathy and heart failure indicating that I was successful in inducing cardiac dysfunction *in vitro*. This study provides the preliminary results necessary for the construction of a microfluidic device to recapitulate the vascular microenvironment to better characterize and investigate vascular related diseases such as SCD.

3.2 Future Works

Microfluidic devices are advantageous over traditional cell culture due to their ability to capture features of the *in vivo* environment such as, cell composition, mechanical stiffness and natural geometry. The aforementioned features are crucial factors in blood disorders like SCD. Mechanotransduction, the chemical signals between cells that regulate cellular behavior, influences cell survival, proliferation, differentiation, adhesion and metabolism. Research over the past two decades has demonstrated the strong influence of substrate stiffness on mechanotransduction. In 1997, Pelham and Wang reported that the stiffness of polyacrylamide gels could regulate focal adhesion and migration of epithelial cells and fibroblast [126]. In addition, the substrate stiffness can drive differentiation of stem cells into specific lineages or maintain pluripotency. In 2006, Engler et al demonstrated that varying the elastic modulus of the substrate directed mesenchymal stem cell differentiation toward bone, neuron or muscle cell lineages [127]. Furthermore, cardiomyocyte mechanotransduction is affected in heart disease via a stiffer environment due to increased cardiomyocyte contractile stress with increased elastic modulus [128]. A stiffer sample had been shown to inhibit contractility in cardiomyocytes and abruptly change spread area in fibroblasts and endothelial cells [129], [130]. Therefore, it is of utmost importance to simulate the *in vivo* stiffness in the development of a physiologically relevant model to investigate cellular behavior and is why we use a 15:1 (527:185) PDMS blend to construct our models.

The natural geometry of a human heart consists of approximately 3,300 capillaries per mm^2 and is vital for nutrient transport and waste elimination [131], [132]. Several methods have been used to mimic the vascularization including decellularized scaffolds, co-culture techniques incorporating endothelial cells and cardiomyocytes, and microfabrication

techniques to design vascular structures [133]–[138]. We are currently investigating methods to effectively fabricate soft PDMS microfluidic devices with varying geometries. Multicompartmental microfluidic devices consisting of endothelial cells, cardiomyocytes and protein coatings will provide an *in vitro* method to capture the intricate cell-cell, cell-ECM and cell-integrin interactions that contribute to cardiomyopathies. The ultimate goal of this research is to develop a multicompartmental microfluidic device to mimic the vasculopathy to improve our understanding of the pathophysiological mechanisms surrounding SCD and identify novel mechanisms for therapeutic targets to improve not only life expectancy, but also the quality of life.

REFERENCES

[1] J. B. Herrick, “Peculiar elongated and sickle-shaped red blood corpuscles in a case of severe anemia,” *Arch. Intern. Med.*, 1910.

[2] L. Pauling, H. A. Itano, S. J. Singer, and I. C. Wells, “Sickle cell anemia, a molecular disease,” *Science (80-.).*, vol. 110, no. 2865, pp. 543–548, 1949.

[3] M. P.T., N. A.C., and W. R.E., “Current management of sickle cell anemia,” *Cold Spring Harb. Perspect. Med.*, vol. 3, no. 8, pp. 1–18, 2013.

[4] G. R. Serjeant, “The Natural History of Sickle Cell Disease,” *Cold Spring Harb. Perspect. Med.*, vol. 3, no. 10, pp. a011783–a011783, Oct. 2013.

[5] M. H. Steinberg, “Sickle Cell Anemia, the First Molecular Disease: Overview of Molecular Etiology, Pathophysiology, and Therapeutic Approaches,” *Sci. World J.*, 2008.

[6] S. Chakravorty and T. N. Williams, “Sickle cell disease: a neglected chronic disease of increasing global health importance.,” *Arch. Dis. Child.*, vol. 100, no. 1, pp. 48–53, Jan. 2015.

[7] K. Wailoo, “Sickle Cell Disease — A History of Progress and Peril,” *N. Engl. J. Med.*, vol. 376, no. 9, pp. 805–807, Mar. 2017.

[8] R. N. Pittman, *Regulation of Tissue Oxygenation Second Edition*. 2016.

[9] G. J. Kato *et al.*, “Sickle cell disease,” *Nat. Rev. Dis. Prim.*, vol. 4, p. 18010, Mar. 2018.

[10] V. Poletti *et al.*, “Pre-clinical Development of a Lentiviral Vector Expressing the Anti-sickling βAS3 Globin for Gene Therapy for Sickle Cell Disease,” *Mol. Ther. - Methods Clin. Dev.*, vol. 11, pp. 167–179, Dec. 2018.

[11] G. R. Serjeant, “The natural history of sickle cell disease.,” *Cold Spring Harb. Perspect. Med.*, vol. 3, no. 10, p. a011783, Oct. 2013.

[12] S. Demirci, N. Uchida, and J. F. Tisdale, “Gene therapy for sickle cell disease: An update,” *Cytotherapy*, vol. 20, no. 7, pp. 899–910, Jul. 2018.

[13] G. J. Kato *et al.*, “Sickle cell disease,” *Nat. Rev. Dis. Prim.*, vol. 4, no. 1, p. 18010, Jun. 2018.

[14] P. J. Griffin *et al.*, "The genetics of hemoglobin A2 regulation in sickle cell anemia," *Am. J. Hematol.*, 2014.

[15] A. Ashley-Koch, Q. Yang, and R. S. Olney, "Sickle hemoglobin (HbS) allele and sickle cell disease: a HuGE review.," *Am. J. Epidemiol.*, vol. 151, no. 9, pp. 839–45, May 2000.

[16] G. Tsaras, A. Owusu-Ansah, F. O. Boateng, and Y. Amoateng-Adjepong, "Complications Associated with Sickle Cell Trait: A Brief Narrative Review," *Am. J. Med.*, vol. 122, no. 6, pp. 507–512, Jun. 2009.

[17] V. Podduturi and J. M. Guileyardo, "Sickle Cell Trait as a Contributory Cause of Death in Natural Disease," *J. Forensic Sci.*, vol. 60, no. 3, pp. 807–811, May 2015.

[18] E. N. Chirico and V. Pialoux, "Role of oxidative stress in the pathogenesis of sickle cell disease," *IUBMB Life*, vol. 64, no. 1, pp. 72–80, Jan. 2012.

[19] D. Manwani and P. S. Frenette, "Vaso-occlusion in sickle cell disease: pathophysiology and novel targeted therapies.," *Blood*, vol. 122, no. 24, pp. 3892–8, Dec. 2013.

[20] A. Piccin *et al.*, "Insight into the complex pathophysiology of sickle cell anaemia and possible treatment," *Eur. J. Haematol.*, vol. 102, no. 4, pp. 319–330, Apr. 2019.

[21] L. Belhassen *et al.*, "Endothelial dysfunction in patients with sickle cell disease is related to selective impairment of shear stress-mediated vasodilation," *Blood*, 2001.

[22] A. K. Mack and G. J. Kato, "Sickle cell disease and nitric oxide: a paradigm shift?," *Int. J. Biochem. Cell Biol.*, vol. 38, no. 8, pp. 1237–43, 2006.

[23] E. Buys and P. Sips, "New insights into the role of soluble guanylate cyclase in blood pressure regulation.," *Curr. Opin. Nephrol. Hypertens.*, vol. 23, no. 2, pp. 135–42, Mar. 2014.

[24] V. Brousse, P. Buffet, and D. Rees, "The spleen and sickle cell disease: the sick(led) spleen," *Br. J. Haematol.*, vol. 166, no. 2, pp. 165–176, Jul. 2014.

[25] S. G. Ahmed, "The role of infection in the pathogenesis of vaso-occlusive crisis in patients with sickle cell disease.," *Mediterr. J. Hematol. Infect. Dis.*, vol. 3, no. 1, p. e2011028, 2011.

[26] S. L. Leikin, D. Gallagher, T. R. Kinney, D. Sloane, P. Klug, and W. Rida, "Mortality in children and adolescents with sickle cell disease. Cooperative Study of Sickle Cell Disease.," *Pediatrics*, vol. 84, no. 3, pp. 500–508, 1989.

[27] O. S. Platt *et al.*, "Mortality In Sickle Cell Disease -- Life Expectancy and Risk Factors for Early Death," *N. Engl. J. Med.*, vol. 330, no. 23, pp. 1639–1644, 1994.

[28] O. O. Ilesanmi, “Pathological basis of symptoms and crises in sickle cell disorder: implications for counseling and psychotherapy.,” *Hematol. Rep.*, vol. 2, no. 1, p. e2, Jan. 2010.

[29] T. M. Ryan, D. J. Ciavatta, and T. M. Townes, “Knockout-Transgenic Mouse Model of Sickle Cell Disease,” vol. 278, no. October, pp. 873–877, 1997.

[30] A. A. Desai *et al.*, “Mechanistic insights and characterization of sickle cell disease-associated cardiomyopathy,” *Circ. Cardiovasc. Imaging*, vol. 7, no. 3, pp. 430–437, 2014.

[31] H. Tran, M. Gupta, and K. Gupta, “Targeting novel mechanisms of pain in sickle cell disease,” *Blood*, vol. 130, no. 22, pp. 2377–2385, Nov. 2017.

[32] B. Lutz, S. E. Meiler, A. Bekker, and Y.-X. Tao, “Updated Mechanisms of Sickle Cell Disease-Associated Chronic pain.,” *Transl. Perioper. pain Med.*, vol. 2, no. 2, pp. 8–17, Jul. 2015.

[33] M. L. Weber *et al.*, “Morphine promotes renal pathology in sickle mice.,” *Int. J. Nephrol. Renovasc. Dis.*, vol. 5, pp. 109–18, 2012.

[34] P. T. McGann, A. C. Nero, and R. E. Ware, “Current management of sickle cell anemia,” *Cold Spring Harb. Perspect. Med.*, 2013.

[35] F. A. Ferrone, “Sickle cell disease: Its molecular mechanism and the one drug that treats it,” *Int. J. Biol. Macromol.*, vol. 93, pp. 1168–1173, 2016.

[36] V. G. Sankaran and S. H. Orkin, “The switch from fetal to adult hemoglobin,” *Cold Spring Harb. Perspect. Med.*, vol. 3, no. 1, 2013.

[37] D. K. Kau, E. Finnegan, and G. A. Barabino, “Sickle red cell-endothelium interactions,” *Microcirculation*. 2009.

[38] L. E. Crosby, L. M. Shook, R. E. Ware, and W. B. Brinkman, “Shared decision making for hydroxyurea treatment initiation in children with sickle cell anemia,” *Pediatric Blood and Cancer*, 2015.

[39] N. Conran, “Prospects for early investigational therapies for sickle cell disease,” *Expert Opin. Investig. Drugs*, 2015.

[40] R. K. Agrawal, R. K. Patel, V. Shah, L. Nainiwal, and B. Trivedi, “Hydroxyurea in sickle cell disease: Drug review,” *Indian Journal of Hematology and Blood Transfusion*. 2014.

[41] C. Hoppe and L. Neumayr, “Sickle Cell Disease: Monitoring, Current Treatment, and Therapeutics Under Development,” *Hematol. Oncol. Clin. North Am.*, vol. 33, no. 3, pp. 355–371, Jun. 2019.

[42] Y. Niihara *et al.*, "A Phase 3 Trial of l -Glutamine in Sickle Cell Disease," *N. Engl. J.Med.*, vol. 379, no. 3, pp. 226–235, Jul. 2018.

[43] T. R. Riley, A. Boss, P. Candidate, D. Mcclain, P. Candidate, and T. T. Riley, "Review of Medication Therapy for the Prevention of Sickle Cell Crisis," vol. 43, no. 7, pp. 417–422, 2018.

[44] S. Kapoor, J. A. Little, and L. H. Pecker, "Advances in the Treatment of Sickle Cell Disease," *Mayo Clinic Proceedings*. 2018.

[45] A. Matte, F. Zorzi, F. Mazzi, E. Federti, O. Olivieri, and L. De Franceschi, "New Therapeutic Options for the Treatment of Sickle Cell Disease.," *Mediterr. J. Hematol. Infect. Dis.*, vol. 11, no. 1, p. e2019002, 2019.

[46] P. R. B. Evora, P. M. Evora, A. C. Celotto, A. J. Rodrigues, and E. E. Joviliano, "Cardiovascular therapeutics targets on the NO-sGC-cGMP signaling pathway: a critical overview.," *Curr. Drug Targets*, vol. 13, no. 9, pp. 1207–14, Aug. 2012.

[47] C. A. Head *et al.*, "Beneficial effects of nitric oxide breathing in adult patients with sickle cell crisis," *Am. J. Hematol.*, vol. 85, no. 10, pp. 800–802, Aug. 2010.

[48] D. L. Weiner, P. L. Hibberd, P. Betit, A. B. Cooper, C. A. Botelho, and C. Brugnara, "Preliminary assessment of inhaled nitric oxide for acute vaso-occlusive crisis in pediatric patients with sickle cell disease.," *JAMA*, vol. 289, no. 9, pp. 1136–42, Mar. 2003.

[49] M. T. Gladwin *et al.*, "Nitric oxide for inhalation in the acute treatment of sickle cell pain crisis: a randomized controlled trial.," *JAMA*, vol. 305, no. 9, pp. 893–902, Mar. 2011.

[50] F. Ichinose, J. D. Roberts, and W. M. Zapol, "Inhaled Nitric Oxide," *Circulation*, vol. 109, no. 25, pp. 3106–3111, Jun. 2004.

[51] N. Conran and L. Torres, "cGMP modulation therapeutics for sickle cell disease," *Exp. Biol. Med.*, vol. 244, no. 2, pp. 132–146, Feb. 2019.

[52] C. R. Morris *et al.*, "Dysregulated Arginine Metabolism, Hemolysis-Associated Pulmonary Hypertension, and Mortality in Sickle Cell Disease," *JAMA*, vol. 294, no. 1, p. 81, Jul. 2005.

[53] C. R. Morris, "Alterations of the Arginine Metabolome in Sickle Cell Disease," *Hematol. Oncol. Clin. North Am.*, vol. 28, no. 2, pp. 301–321, Apr. 2014.

[54] C. Morris and N. Bakshi, "The role of the arginine metabolome in pain: implications for sickle cell disease," *J. Pain Res.*, vol. 9, p. 167, Mar. 2016.

[55] C. R. Morris *et al.*, "A randomized, placebo-controlled trial of arginine therapy for the treatment of children with sickle cell disease hospitalized with vaso-occlusive pain episodes.," *Haematologica*, vol. 98, no. 9, pp. 1375–82, Sep. 2013.

[56] E. S. Buys *et al.*, "Discovery and development of next generation sGC stimulators with diverse multidimensional pharmacology and broad therapeutic potential," *Nitric Oxide*, vol. 78, pp. 72–80, Aug. 2018.

[57] J.-P. Stasch and O. V. Evgenov, "Soluble Guanylate Cyclase Stimulators in Pulmonary Hypertension," in *Handbook of experimental pharmacology*, vol. 218, 2013, pp. 279–313.

[58] J. Miyashiro *et al.*, "The Effect of the Soluble Guanylyl Cyclase Stimulator Olinciguat on γ-Globin Gene Induction in K562 Cells," *Blood*, vol. 132, no. Suppl 1, pp. 1078–1078, Nov. 2018.

[59] K. I. Ataga *et al.*, "Crizanlizumab for the Prevention of Pain Crises in Sickle Cell Disease," *N. Engl. J. Med.*, 2016.

[60] A. Kutlar *et al.*, "Effect of crizanlizumab on pain crises in subgroups of patients with sickle cell disease: A SUSTAIN study analysis," *Am. J. Hematol.*, vol. 94, no. 1, pp. 55–61, Jan. 2019.

[61] J. Kanter *et al.*, "Ticagrelor does not impact patient-reported pain in young adults with sickle cell disease: a multicentre, randomised phase II b study," *Br. J. Haematol.*, vol. 184, no. 2, pp. 269–278, Jan. 2019.

[62] W. A. Eaton and H. F. Bunn, "Treating sickle cell disease by targeting HbS polymerization.," *Blood*, vol. 129, no. 20, pp. 2719–2726, 2017.

[63] J. Howard *et al.*, "A phase 1/2 ascending dose study and open-label extension study of voxelotor in patients with sickle cell disease.," *Blood*, vol. 133, no. 17, pp. 1865–1875, Apr. 2019.

[64] L. J. Estcourt, P. M. Fortin, S. Hopewell, and M. Trivella, "Red blood cell transfusion to treat or prevent complications in sickle cell disease: an overview of Cochrane reviews.," *Cochrane database Syst. Rev.*, vol. 2016, no. 2, Feb. 2016.

[65] S. T. Chou, "Transfusion therapy for sickle cell disease: a balancing act," *Hematology*, vol. 2013, no. 1, pp. 439–446, Dec. 2013.

[66] D. C. Rees, S. Robinson, and J. Howard, "How I manage red cell transfusions in patients with sickle cell disease," *Br. J. Haematol.*, vol. 180, no. 4, pp. 607–617, Feb. 2018.

[67] R. S. Nickel *et al.*, "Impact of red blood cell alloimmunization on sickle cell disease mortality: a case series," *Transfusion*, vol. 56, no. 1, pp. 107–114, Jan. 2016.

[68] A. M. Writers, "Both prevention and treatment are important when managing sickle cell disease," *Drugs Ther. Perspect.*, vol. 30, no. 12, pp. 411–416, Dec. 2014.

[69] A. T. W. Cheung *et al.*, "Exchange Transfusion Therapy and Its Effects on Real-time Microcirculation in Pediatric Sickle Cell Anemia Patients," *J. Pediatr. Hematol. / Oncol.*, vol. 34, no. 3, pp. 169–174, Apr. 2012.

[70] M. de Montalembert *et al.*, "Are the risks of treatment to cure a child with severe sickle cell disease too high?," *BMJ*, vol. 359, p. j5250, Nov. 2017.

[71] M. Bhatia and S. Sheth, "Hematopoietic stem cell transplantation in sickle cell disease: patient selection and special considerations.," *J. Blood Med.*, vol. 6, pp. 229–38, 2015.

[72] M. D. Hoban *et al.*, "Correction of the sickle cell disease mutation in human hematopoietic stem/progenitor cells.," *Blood*, vol. 125, no. 17, pp. 2597–604, Apr. 2015.

[73] D. P. Dever *et al.*, "CRISPR/Cas9 β-globin gene targeting in human haematopoietic stem cells," *Nature*, vol. 539, no. 7629, pp. 384–389, Nov. 2016.

[74] C.-H. Wu, S. Mohammadmoradi, J. Z. Chen, H. Sawada, A. Daugherty, and H. S. Lu, "Renin-Angiotensin System and Cardiovascular Functions.," *Arterioscler. Thromb. Vasc. Biol.*, vol. 38, no. 7, pp. e108–e116, Jul. 2018.

[75] W. C. De Mello and A. H. Danser, "Angiotensin II and the heart : on the intracrine renin-angiotensin system.," *Hypertens. (Dallas, Tex. 1979)*, vol. 35, no. 6, pp. 1183–8, Jun. 2000.

[76] K. M. Baker, G. W. Booz, and D. E. Dostal, "Cardiac Actions of Angiotensin II: Role of an Intracardiac Renin-Angiotensin System," *Annu. Rev. Physiol.*, vol. 54, no. 1, pp. 227–241, Oct. 1992.

[77] S. Ahmad *et al.*, "Primacy of cardiac chymase over angiotensin converting enzyme as an angiotensin-(1-12) metabolizing enzyme.," *Biochem. Biophys. Res. Commun.*, vol. 478, no. 2, pp. 559–64, 2016.

[78] M. Ihara *et al.*, "Increased Chymase-Dependent Angiotensin II Formation in Human Atherosclerotic Aorta," *Hypertension*, vol. 33, no. 6, pp. 1399–1405, Jun. 1999.

[79] A. Nehme, F. A. Zouein, Z. D. Zayeri, and K. Zibara, "An Update on the Tissue Renin Angiotensin System and Its Role in Physiology and Pathology," *J. Cardiovasc. Dev. Dis.*, vol. 6, no. 2, p. 14, Mar. 2019.

[80] F. M. Bumpus *et al.*, "Nomenclature for angiotensin receptors. A report of the Nomenclature Committee of the Council for High Blood Pressure Research.," *Hypertension*, vol. 17, no. 5, pp. 720–721, May 1991.

[81] C. Dasgupta and L. Zhang, "Angiotensin II receptors and drug discovery in cardiovascular disease.," *Drug Discov. Today*, vol. 16, no. 1–2, pp. 22–34, Jan. 2011.

[82] T. B. Rogers, S. T. Gaa, and I. S. Allen, “Identification and characterization of functional angiotensin II receptors on cultured heart myocytes.,” *J. Pharmacol. Exp. Ther.*, vol. 236, no. 2, pp. 438–44, Feb. 1986.

[83] M. de Gasparo, K. J. Catt, T. Inagami, J. W. Wright, and T. Unger, “International union of pharmacology. XXIII. The angiotensin II receptors.,” *Pharmacol. Rev.*, vol. 52, no. 3, pp. 415–72, Sep. 2000.

[84] S. Kim and H. Iwao, “Molecular and cellular mechanisms of angiotensin II-mediated cardiovascular and renal diseases.,” *Pharmacol. Rev.*, vol. 52, no. 1, pp. 11–34, Mar. 2000.

[85] S. J. Forrester *et al.*, “Angiotensin II Signal Transduction: An Update on Mechanisms of Physiology and Pathophysiology,” *Physiol. Rev.*, vol. 98, no. 3, pp. 1627–1738, Jul. 2018.

[86] L. C. Matavelli and H. M. Siragy, “AT2 receptor activities and pathophysiological implications.,” *J. Cardiovasc. Pharmacol.*, vol. 65, no. 3, pp. 226–32, Mar. 2015.

[87] W. C. De Mello and E. D. Frohlich, “Clinical Perspectives and Fundamental Aspects of Local Cardiovascular and Renal Renin-Angiotensin Systems,” *Front. Endocrinol. (Lausanne).*, vol. 5, p. 16, 2014.

[88] F.-M. Jazmín, L.-M. Diego, and M.-A. Luisa, “Function of renin angiotensin system on heart failure,” *J. Integr. Cardiol.*, vol. 2, no. 5, 2016.

[89] R. A. Gonzalez-Villalobos *et al.*, “Intrarenal mouse renin-angiotensin system during ANG II-induced hypertension and ACE inhibition.,” *Am. J. Physiol. Renal Physiol.*, vol. 298, no. 1, pp. F150-7, Jan. 2010.

[90] M.-Q. Dang *et al.*, “Gene expression profile in the early stage of angiotensin II-induced cardiac remodeling: a time series microarray study in a mouse model.,” *Cell. Physiol. Biochem.*, vol. 35, no. 2, pp. 467–76, 2015.

[91] A. E. Loot, J. G. Schreiber, B. Fisslthaler, and I. Fleming, “Angiotensin II impairs endothelial function via tyrosine phosphorylation of the endothelial nitric oxide synthase,” *J. Exp. Med.*, vol. 206, no. 13, pp. 2889–2896, Dec. 2009.

[92] W.-J. Li *et al.*, “‘Angiotensin II memory’ contributes to the development of hypertension and vascular injury via activation of NADPH oxidase,” *Life Sci.*, vol. 149, pp. 18–24, 2016.

[93] D. Zablocki and J. Sadoshima, “Angiotensin II and Oxidative Stress in the Failing Heart,” *Antioxid. Redox Signal.*, vol. 19, no. 10, pp. 1095–1109, 2013.

[94] S. J. Watkins, G. M. Borthwick, R. Oakenfull, A. Robson, and H. M. Arthur, "Angiotensin II-induced cardiomyocyte hypertrophy in vitro is TAK1-dependent and Smad2/3-independent," *Hypertens. Res.*, vol. 35, no. 4, pp. 393–398, Apr. 2012.

[95] N. Kim *et al.*, "Angiotensin II affects inflammation mechanisms via AMPK-related signalling pathways in HL-1 atrial myocytes," *Sci. Rep.*, vol. 7, no. 1, p. 10328, Dec. 2017.

[96] R. E. Horton *et al.*, "Angiotensin II Induced Cardiac Dysfunction on a Chip," *PLoS One*, vol. 11, no. 1, p. e0146415, Jan. 2016.

[97] A. E. Loot, J. G. Schreiber, B. Fisslthaler, and I. Fleming, "Angiotensin II impairs endothelial function via tyrosine phosphorylation of the endothelial nitric oxide synthase," *J. Exp. Med.*, vol. 206, no. 13, pp. 2889–2896, Dec. 2009.

[98] T. Watanabe, T. A. Barker, and B. C. Berk, "Angiotensin II and the Endothelium," *Hypertension*, vol. 45, no. 2, pp. 163–169, Feb. 2005.

[99] G. Lu, S. Xu, L. Peng, Z. Huang, Y. Wang, and X. Gao, "Angiotensin II upregulates Kv1.5 expression through ROS-dependent transforming growth factor-beta1 and extracellular signal-regulated kinase 1/2 signalings in neonatal rat atrial myocytes," *Biochem. Biophys. Res. Commun.*, vol. 454, no. 3, pp. 410–416, 2014.

[100] Z. Wu, F. Dai, W. Ren, H. Liu, B. Li, and J. Chang, "Angiotensin II induces apoptosis of human pulmonary microvascular endothelial cells in acute aortic dissection complicated with lung injury patients through modulating the expression of monocyte chemoattractant protein-1," *Am J Transl Res*, vol. 8, no. 1, pp. 28–36, 2016.

[101] S. Xu, H. Zhi, X. Hou, R. A. Cohen, and B. Jiang, "IκBβ attenuates angiotensin II-induced cardiovascular inflammation and fibrosis in mice," *Hypertension*, vol. 58, no. 2, pp. 310–316, Oct. 2011.

[102] E. A. Manci, C. A. Hillery, C. A. Bodian, Z. G. Zhang, G. A. Lutty, and B. S. Coller, "Pathology of Berkeley sickle cell mice: similarities and differences with human sickle cell disease.," *Blood*, vol. 107, no. 4, pp. 1651–8, Feb. 2006.

[103] T. M. Ryan, D. J. Ciavatta, and T. M. Townes, "Knockout-transgenic mouse model of sickle cell disease.," *Science*, vol. 278, no. 5339, pp. 873–6, Oct. 1997.

[104] J. Lei, B. Benson, H. Tran, S. F. Ofori-Acquah, and K. Gupta, "Comparative Analysis of Pain Behaviours in Humanized Mouse Models of Sickle Cell Anemia," *PLoS One*, vol. 11, no. 8, p. e0160608, Aug. 2016.

[105] A. W. Feinberg *et al.*, "Controlling the contractile strength of engineered cardiac muscle by hierarchal tissue architecture," *Biomaterials*, vol. 33, no. 23, pp. 5732–5741, Aug. 2012.

[106] M.-A. Bray, S. P. Sheehy, and K. K. Parker, "Sarcomere alignment is regulated by myocyte shape," *Cell Motil. Cytoskeleton*, vol. 65, no. 8, pp. 641–651, Aug. 2008.

[107] W. J. Adams, T. Pong, N. A. Geisse, S. P. Sheehy, B. Diop-Frimpong, and K. K. Parker, "Engineering design of a cardiac myocyte," *J. Comput. Mater. Des.*, vol. 14, no. 1, pp. 19–29, Apr. 2007.

[108] T. D. Schmittgen and K. J. Livak, "Analyzing real-time PCR data by the comparative CT method," *Nat. Protoc.*, vol. 3, no. 6, pp. 1101–1108, Jun. 2008.

[109] J. Zhao *et al.*, "Identification of target genes in cardiomyopathy with fibrosis and cardiac remodeling," *J. Biomed. Sci.*, vol. 25, no. 1, p. 63, Dec. 2018.

[110] F. Cambronero, F. Marin, V. Roldan, D. Hernandez-Romero, M. Valdes, and G. Y. H. Lip, "Biomarkers of pathophysiology in hypertrophic cardiomyopathy: implications for clinical management and prognosis," *Eur. Heart J.*, vol. 30, no. 2, pp. 139–151, May 2008.

[111] V. F. M. Segers, D. L. Brutsaert, and G. W. De Keulenaer, "Cardiac Remodeling: Endothelial Cells Have More to Say Than Just NO.," *Front. Physiol.*, vol. 9, p. 382, 2018.

[112] Y. Liu *et al.*, "Angiotensin II Stimulation In Vitro Induces Hypertrophy of Normal and Postinfarcted Ventricular Myocytes," *Circ. Res.*, vol. 82, no. 11, pp. 1145–1159, Jun. 1998.

[113] L. Gullestad, T. Ueland, L. E. Vinge, A. Finsen, A. Yndestad, and P. Aukrust, "Inflammatory Cytokines in Heart Failure: Mediators and Markers," *Cardiology*, vol. 122, no. 1, pp. 23–35, 2012.

[114] N. G. Frangogiannis, "The inflammatory response in myocardial injury, repair, and remodelling.," *Nat. Rev. Cardiol.*, vol. 11, no. 5, pp. 255–65, May 2014.

[115] V. Stangl, G. Baumann, K. Stangl, and S. B. Felix, "Negative inotropic mediators released from the heart after myocardial ischaemia–reperfusion," *Cardiovasc. Res.*, vol. 53, no. 1, pp. 12–30, Jan. 2002.

[116] A. Angelini, Z. Li, M. Mericskay, and J.-F. Decaux, "Regulation of Connective Tissue Growth Factor and Cardiac Fibrosis by an SRF/MicroRNA-133a Axis.," *PLoS One*, vol. 10, no. 10, p. e0139858, 2015.

[117] C.-K. Wu *et al.*, "Connective tissue growth factor and cardiac diastolic dysfunction: human data from the Taiwan Diastolic Heart Failure Registry and molecular basis by cellular and animal models," *Eur. J. Heart Fail.*, vol. 16, no. 2, pp. 163–172, Feb. 2014.

[118] A. Gandaglia *et al.*, "Cardiomyocytes in vitro adhesion is actively influenced by biomimetic synthetic peptides for cardiac tissue engineering.," *Tissue Eng. Part A*, vol. 18, no. 7–8, pp. 725–36, Apr. 2012.

[119] I. A. Sergeeva and V. M. Christoffels, "Regulation of expression of atrial and brain natriuretic peptide, biomarkers for heart development and disease," *Biochim. Biophys. Acta - Mol. Basis Dis.*, vol. 1832, no. 12, pp. 2403–2413, Dec. 2013.

[120] G. Yan *et al.*, "Orphan Nuclear Receptor Nur77 Inhibits Cardiac Hypertrophic Response to Beta-Adrenergic Stimulation," *Mol. Cell. Biol.*, vol. 35, no. 19, pp. 3312–3323, Oct. 2015.

[121] M. Cui *et al.*, "Orphan Nuclear Receptor Nur77 Inhibits Angiotensin II–Induced Vascular Remodeling via Downregulation of β-Catenin," *Hypertension*, vol. 67, no. 1, pp. 153–162, Jan. 2016.

[122] Y. Y. Grinberg, M. E. Dibbern, V. A. Levasseur, and R. P. Kraig, "Insulin-like growth factor-1 abrogates microglial oxidative stress and TNF-α responses to spreading depression.," *J. Neurochem.*, vol. 126, no. 5, pp. 662–72, Sep. 2013.

[123] Y. Y. Grinberg, W. van Drongelen, and R. P. Kraig, "Insulin-like growth factor-1 lowers spreading depression susceptibility and reduces oxidative stress.," *J. Neurochem.*, vol. 122, no. 1, pp. 221–9, Jul. 2012.

[124] N. Zhang, B. T. Andresen, and C. Zhang, "Inflammation and reactive oxygen species in cardiovascular disease.," *World J. Cardiol.*, vol. 2, no. 12, pp. 408–10, Dec. 2010.

[125] B. C. Berk, K. Fujiwara, and S. Lehoux, "ECM remodeling in hypertensive heart disease," *J. Clin. Invest.*, vol. 117, no. 3, pp. 568–575, Mar. 2007.

[126] R. J. Pelham and Y. -l. Wang, "Cell locomotion and focal adhesions are regulated by substrate flexibility," *Proc. Natl. Acad. Sci.*, vol. 94, no. 25, pp. 13661–13665, Dec. 1997.

[127] A. J. Engler, S. Sen, H. L. Sweeney, and D. E. Discher, "Matrix Elasticity Directs Stem Cell Lineage Specification," *Cell*, vol. 126, no. 4, pp. 677–689, Aug. 2006.

[128] P. Pandey *et al.*, "Cardiomyocytes Sense Matrix Rigidity through a Combination of Muscle and Non-muscle Myosin Contractions," *Dev. Cell*, Jan. 2018.

[129] P. Pandey *et al.*, "Cardiomyocytes Sense Matrix Rigidity through a Combination of Muscle and Non-muscle Myosin Contractions.," *Dev. Cell*, vol. 44, no. 3, pp. 326-336.e3, Jan. 2018.

[130] L. B. Hazeltine *et al.*, "Effects of Substrate Mechanics on Contractility of Cardiomyocytes Generated from Human Pluripotent Stem Cells," *Int. J. Cell Biol.*, vol. 2012, pp. 1–13, May 2012.

[131] J. T. Roberts and J. T. Wearn, "Quantitative changes in the capillary-muscle relationship in human hearts during normal growth and hypertrophy," *Am. Heart J.*, vol. 21, no. 5, pp. 617–633, May 1941.

[132] N. Kaneko, R. Matsuda, M. Toda, and K. Shimamoto, "Three-dimensional reconstruction of the human capillary network and the intramyocardial micronecrosis," *Am. J. Physiol. Circ. Physiol.*, vol. 300, no. 3, pp. H754–H761, Mar. 2011.

[133] H. C. Ott *et al.*, "Perfusion-decellularized matrix: using nature's platform to engineer a bioartificial heart," *Nat. Med.*, vol. 14, no. 2, pp. 213–221, Feb. 2008.

[134] S. Levenberg *et al.*, "Engineering vascularized skeletal muscle tissue," *Nat. Biotechnol.*, vol. 23, no. 7, pp. 879–884, Jul. 2005.

[135] H. Sekine *et al.*, "Endothelial Cell Coculture Within Tissue-Engineered Cardiomyocyte Sheets Enhances Neovascularization and Improves Cardiac Function of Ischemic Hearts," *Circulation*, vol. 118, no. 14_suppl_1, pp. S145–S152, Sep. 2008.

[136] S. Kaihara *et al.*, "Silicon Micromachining to Tissue Engineer Branched Vascular Channels for Liver Fabrication," *Tissue Eng.*, vol. 6, no. 2, pp. 105–117, Apr. 2000.

[137] A. P. Golden and J. Tien, "Fabrication of microfluidic hydrogels using molded gelatin as a sacrificial element," *Lab Chip*, vol. 7, no. 6, p. 720, Jun. 2007.

[138] M. D. S. Frame and I. H. Sarelius, "A System for Culture of Endothelial Cells in 20–50-μm Branching Tubes," *Microcirculation*, vol. 2, no. 4, pp. 377–385, Jan. 1995.